Journal of Structural Geology 182 (2024) 105102

Contents lists available at ScienceDirect

Journal of Structural Geology

journal homepage: www.elsevier.com/locate/jsg

Influence of a rigid backstop on the flow pattern during thrusting of the supracrustal Balsfjord Series of the North Norwegian Caledonides

Stephan M. Höpfl [a,*], Jiří Konopásek [a,b], Jiří Sláma [c]

[a] Department of Geosciences, UiT The Arctic University of Norway, Dramsvegen 201, 9010, Tromsø, Norway
[b] Czech Geological Survey, Klárov 3, 118 21, Praha, 1, Czech Republic
[c] Institute of Geology of the Czech Academy of Sciences, Rozvojová 269, 165 00, Praha, 6, Czech Republic

ARTICLE INFO

Keywords:
Rotation of lineation
Escape tectonics
Nappe thrusting
Balsfjord Series
North Norwegian Caledonides

ABSTRACT

The Caledonian evolution of the low–medium grade Balsfjord Series (Troms, Northern Norway) is characterized by four sets of deformation structures that developed progressively during burial and exhumation from underneath the high-grade Nakkedal and Tromsø nappe complexes. The Balsfjord Series commonly displays top-to-the SSE–SE directed movement during the development of the main metamorphic fabric with local folding at different evolutionary stages. However, we document a structural horizon within the Balsfjord Series showing a strong reorientation of the regional stretching lineation from NW–SE to E–W and finally NE–SW. This rotation occurred during exhumation and is interpreted as a lateral escape mechanism resulting from thrusting of the rheologically soft Balsfjord Series against the rigid backstop of the Lyngen Magmatic Complex and the Mauken Window basement.

U–Pb dating of titanite from shear zones within the West Troms Basement Complex yielded an age of 429 ± 5 Ma interpreted as the age of thrusting of the overlying Balsfjord Series. To account for all field relationships with the overlying and underlying units, we interpret the tectonic evolution of the Balsfjord Series as a result of an interaction of two sutures active at ca. 430 Ma.

1. Introduction

Crustal thickening and the transport of large-scale nappe units (Termier, 1922) are some of the most dominant features in collisional orogens representing first-order tectonic processes governing the formation and modification of upper to lower orogenic crust (e.g., Schulmann et al., 1994; Escher and Beaumont, 1997; Van Hinsbergen et al., 2005). Internally, such orogens show a distinct tectonic zonation characterized by several allochthonous units, which occasionally travel hundreds of kilometres (Lundmark et al., 2007; Jamieson and Beaumont, 2011; McArthur et al., 2014) onto a mostly stable continental basement (Bird and Dewey, 1970; Dewey et al., 1973; Zhong et al., 2023). Since the recognition of the widespread presence of nappes in orogenic belts, significant efforts were devoted to better understand their kinematics (e.g., Herwegh and Pfiffner, 2005; Bellahsen et al., 2012; Boutoux et al., 2014; Kiss et al., 2020) and to identify the main emplacement mechanisms (e.g. Merle, 1998). The suggested driving forces facilitating nappe transport are either exterior surface forces like heterogenous shearing resulting from tectonic compression (Ramsay et al., 1983; Mohanty and Ramsay, 1994; Bauville et al., 2013; Boutoux et al., 2014; Kiss et al., 2020), extrusion (e.g., Thompson et al., 1997; Beaumont et al., 2001; Schulmann et al., 2008) or interior body forces due to gravity (Merle, 1989; Merle and Guillier, 1989; Turner, 1995). An important factor in understanding the principal movement of nappe allochthons in orogens is the orientation of stretching lineations, which are generally interpreted to form parallel to the main transport direction (e.g., Cloos, 1946; Selverstone, 1988; Ratschbacher et al., 1989; Peterson and Robinson, 1993; Xu et al., 2013). For the Caledonian orogeny in northern Norway, these stretching lineations have been documented to predominantly lie at a high angle to the orogenic fabric (Janák et al., 2012; Faber et al., 2019; Ceccato et al., 2020), although local orogen-parallel lineations were recorded as well (Kirkland et al., 2006).

The North Norwegian Caledonides are currently depicted as an uninterrupted stack of nappe units ranging from the Tromsø and Nakkedal nappes, through the Balsfjord Series and Lyngen Magmatic Complex (LMC) to the underlying Reisa Nappe Complex (RNC) and the Kalak Nappe complex (KNC), which finally overlie the par-autochthonous Dividal Unit and the Baltic Shield (Fig. 1; Janák et al., 2012; Augland

* Corresponding author. Dramsvegen 201, 9010, Tromsø, Norway.
E-mail addresses: stephan.m.hopfl@uit.no (S.M. Höpfl), jiri.konopasek@uit.no (J. Konopásek), slama@gli.cas.cz (J. Sláma).

https://doi.org/10.1016/j.jsg.2024.105102
Received 28 November 2023; Received in revised form 6 March 2024; Accepted 9 March 2024
Available online 17 March 2024

et al., 2014). However, in areas where the offset by post-Caledonian normal faults is negligible, the low–medium grade Balsfjord Series is mapped as directly overlying the Baltica basement (Fareth, 1977; Zwaan et al., 1998, 2009; Velvin et al., 2015), which contradicts the current interpretation of the local tectonostratigraphy. This study examines the structural evolution of the Balsfjord Series in the County of Troms and Finnmark in northern Norway where all the above-mentioned nappe units are exposed. In the southeastern part of the study area (Fig. 1), the Balsfjord Series is comprised of partly fossiliferous low-grade metamorphic rocks (Binns and Matthews, 1981; Bjørlykke and Olaussen, 1981; Anderson et al., 1992; Anderson and Barker, 1999) which directly overlie the upper amphibolite-to granulite-facies rocks of the uppermost RNC (Faber et al., 2019). This large difference in metamorphic conditions between two neighboring units cannot be explained by a simple model of continuous in-sequence thrusting. A similar configuration has been described further south, where the Øse-thrust separates the kyanite-sillimanite bearing gneisses of the Kvernmo nappe from the overlying greenschist-facies rocks of the Øse nappe (Anderson et al., 1992; Anderson and Barker, 1999). We present new structural data and discuss the role of the Balsfjord Series during the assembly of the North Norwegian Caledonian nappe stack. We have identified four phases of progressive deformation that affected the unit during burial and subsequent thrusting. We document a significant rotation of the stretching lineation gradually changing from an orogen-perpendicular to orogen-parallel direction and interpret it as another example of local lateral escape occurring during development of the North Norwegian Caledonian nappe assembly (cf. Kirkland et al., 2006). Our work outlines the role of the Lyngen Magmatic Complex and the underlying basement promontory (the Mauken Window) in the nappe translation of the metasedimentary Balsfjord Series rocks. We also confirm the direct contact of the Balsfjord Series with the underlying West Troms Basement Complex in the northwest and southwest of the study area, as well as the sudden increase in metamorphic conditions between the low-grade parts of the Balsfjord Series with respect to the underlying Reisa Nappe

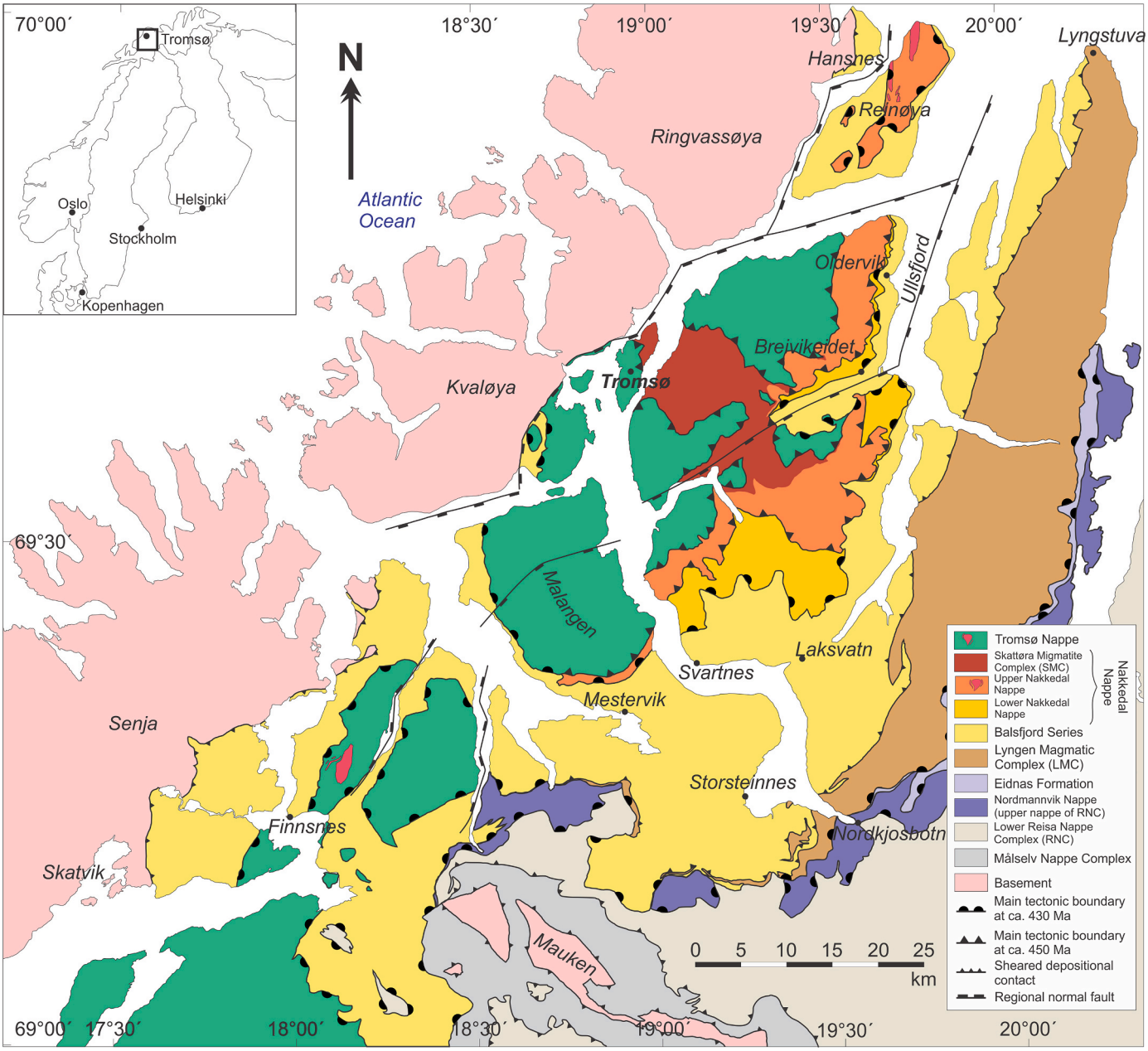

Fig. 1. Simplified geological map of the North Norwegian Caledonides in the area of Troms and Finnmark county, modified from Zwaan et al. (1998).

Complex. Even though both features have been previously documented (see above), their tectonic meaning has not been interpreted. We discuss our results together with previously published data and suggest a structural/tectonic model that reconciles many of the somewhat enigmatic features of the North Norwegian Caledonian nappe assembly.

2. Geological setting

The Caledonian orogen formed during the Ordovician–Devonian as a result of the collision between Laurentia, Baltica and Avalonia and is found on both sides of the northern Atlantic Ocean (Corfu et al., 2014a). Current models of the tectonic evolution of the orogen describe various thrust sheets of variable paleogeographic origin and metamorphic grade, that were exhumed and emplaced onto the Fennoscandian Shield representing a deeply eroded middle–lower crustal basement (Roberts, 2003). Regional works aiming to better understand individual nappe assemblies throughout Norway and Sweden were carried out by various authors from north to south (Andresen et al., 1985, 2014; Bergh and Andresen, 1985; Andersen et al., 1991; Anderson et al., 1992; Anderson and Barker, 1999; Augland et al., 2014; Gee et al., 2014; Marko et al., 2014; McArthur et al., 2014; Rice, 2014; Slagstad et al., 2014) and these local studies have been summarized in several milestone publications that attempted to provide a unifying tectonic model for the entire Scandinavian Caledonides (e.g., Gee, 1975; Gee and Sturt, 1985; Roberts, 2003; Corfu et al., 2014a, 2014b).

The North Norwegian Caledonides in Troms and Finnmark county are represented by several nappe complexes (Fig. 1) that were thrust on top of each other during the final stages of the collision (Gee et al., 2008; Corfu et al., 2014b). These allochthonous units were historically.

labelled as the Lower, Middle, Upper and Uppermost Allochthon (Gee and Sturt, 1985; Roberts et al., 1985; Anderson et al., 1992), however, recent work of Corfu et al. (2014) has discouraged the use of these terms. In the Troms and Finnmark region, the SE–NW tectonic zonation of the orogen is interrupted by a series of regional, post-Caledonian, brittle normal faults (Fig. 1) (Zwaan et al., 1998), along which large parts of the allochthonous units were placed next to the underlying Archean–Paleoproterozoic West Troms Basement Complex (WTBC) (Bergh et al., 2010). From bottom to top the allochthonous units comprise the Dividal Unit (Andresen et al., 2014), the Kalak Nappe Complex (KNC) (Kirkland et al., 2006; Ceccato et al., 2020) and the Reisa Nappe Complex (RNC) (Faber et al., 2019). The latter is overlain by the Lyngen Magmatic Complex (LMC), representing the largest ophiolite complex in the Scandinavian Caledonides with a minimum formation age of 481 ± 6 Ma (Oliver and Krogh, 1995; Kvassnes et al., 2004; Augland et al., 2014) and the metasedimentary Balsfjord Series (Andresen and Bergh, 1985; Bergh and Andresen, 1985; Coker-Dewey et al., 2000). Finally, the Balsfjord Series underlies the Nakkedal Nappe (Zwaan et al., 1998) followed by the uppermost eclogite-bearing Tromsø Nappe (Corfu et al., 2003b; Janák et al., 2013; Fassmer et al., 2020).

Previous works (e.g., Janák et al., 2012; Augland et al., 2014) described this nappe assembly as one uninterrupted sequence from the parautochthonous Dividal Unit up to the Tromsø Nappe. However, major discontinuities in terms of metamorphic and temporal history between the upper part of the RNC and the overlying LMC as well as the Balsfjord Series have been reported (Faber et al., 2019), similar to the continuation of the upper Caledonian tectonic units further south (Anderson et al., 1992; Anderson and Barker, 1999). These discrepancies do not allow to consider the present position of the Caledonian nappes as a result of a simple in-sequence thrusting process. The RNC experienced a polyphase metamorphic history with an anti-clockwise P–T path (Faber et al., 2019). Its uppermost unit called the Nordmannvik Nappe features partial melting in the kyanite stability field (9–11 kbar, 780 °C) at ca. 440 Ma, followed by shearing of the partially molten unit at ca. 432 Ma (9–11 kbar and 700 °C) (Faber et al. 2019). Only little is known about the metamorphic history of the LMC and the Balsfjord Series above, however the latter has been described as a low–medium grade unit with an inverted metamorphic gradient (Andresen et al., 1985; Coker-Dewey et al., 2000; Menegon and Fagereng, 2021). The boundary between the upper RNC to the LMC/Balsfjord Series thus marks a sharp drop in metamorphic conditions, as well as a possible discontinuity in age of the metamorphic peak. In the southern part of the study area (Fig. 1), the LMC is strongly thinned in comparison to its main body in the north, resulting in the Balsfjord Series directly overlying the Nordmannvik Nappe of the RNC. Further south to this contact lie the Målselv Nappe Complex and the Precambrian basement of the Mauken Window consisting of Archean–Palaeoproterozoic supracrustal and intrusive rocks of variable tectonic origin (Bjerkgård et al., 2015).

Similar to the Nordmannvik Nappe of the RNC, the Nakkedal and Tromsø nappes on top of the Balsfjord Series form another high-grade complex in the area (e.g Janák et al., 2012, 2013; Kullerud et al., 2012). Investigation of these two nappes has shown that the Nakkedal Nappe experienced significant partial melting at conditions of >850 °C and >12 kbar (Selbekk et al., 2000; Selbekk and Skjerlie, 2002; Kullerud et al., 2012), while the Tromsø Nappe features rocks that underwent ultrahigh pressure metamorphism (ca. 35 kbar and 750–800C°), (Krogh et al., 1990; Ravna and Roux, 2006; Janák et al., 2012, 2013). The timing of the metamorphic peak in the Nakkedal Nappe is derived from U–Pb dating of titanite from leucocratic veins and leucosomes in the Skattøra Migmatite Complex (Fig. 1) (456 ± 4 Ma, Selbekk et al., 2000). Notably, the timing of metamorphism in the Tromsø Nappe is exclusively known for "exotic" rocks such as eclogites (ca. 449–452 Ma; Corfu et al., 2003b; Fassmer et al., 2020) or carbonatites (ca. 452–455 Ma; Ravna et al., 2017), which are prominent, but limited occurrences within the large nappe unit dominated by metasedimentary rocks. Both the Nakkedal and Tromsø nappes are intruded by small granitic bodies post-dating peak metamorphism in these units (Fig. 1). One of these bodies intruding the Nakkedal nappe yielded a Rb–Sr age of 432 ± 7 Ma (Lindstrøm and Andresen, 1995).

The West Troms Basement Complex (WTBC; (Corfu et al., 2003a; Kullerud et al., 2006; Bergh et al., 2010, 2015; Myhre et al., 2011) in the west of the study area is commonly interpreted as a western continuation of the Fennoscandian Shield (Olesen et al., 1997; Bergh et al., 2010; Paulsen et al., 2021) but may also be in a parautochthonous to allochthonous position to it (Dallmeyer, 1992 and references therein). The Caledonian overprint that the WTBC received during the Caledonian orogeny is considered to be weak or non-existent (Corfu et al., 2003a; Kullerud et al., 2006; Bergh et al., 2015). Although several studies referred to by Dallmeyer (1992) indicate otherwise, these only exist as abstracts (Bergh and Andresen, 1988).

The Balsfjord Series is a fossil-bearing (Binns and Matthews, 1981; Bjørlykke and Olaussen, 1981) low to medium-grade unit (Augland et al., 2014) with inverted metamorphism (Coker-Dewey et al., 2000) that increases from the SE towards the W and NW. It is mainly comprised of garnet micaschists, but also contains quartzites, marbles, greenschists, conglomerates and gneisses together with rare occurrences of mafic lenses (Zwaan et al., 1998). The deposition age of parts of the Balsfjord Series has been constrained by Llandoverian fossils (444-433 Ma; Binns and Matthews, 1981; Bjørlykke and Olaussen, 1981), also providing a maximum age of metamorphism. $^{40}Ar/^{39}Ar$ ages of hornblende (432 ± 2 Ma) and muscovite (417 ± 1 Ma and 424 ± 1 Ma) likely provide the timing close to peak metamorphism and subsequent cooling, respectively (Dallmeyer and Andresen, 1992). There are no precise absolute ages for the depositional time of the Balsfjord Series or its metamorphic peak. Augland et al. (2014) performed U–Pb dating of

zircons in a small granitic body that is late syn-tectonic with respect to the fabric of the host Balsfjord metapelites. One of the grains dated at 425 ± 1 Ma was interpreted to represent the crystallization age of the intrusion (Augland et al., 2014). There have been several studies concerning the structural evolution of the Balsfjord Series (e.g., Andresen and Bergh, 1985; Andresen et al., 1985; Bergh and Andresen, 1985; Coker-Dewey et al., 2000) however back then several of the above-mentioned units were defined differently or have not been defined at all (Nakkedal Nappe). This includes the Balsfjord Series with its westernmost parts being assigned to a different unit entirely (Senja Nappe) or not being mapped yet (Andresen and Bergh, 1985). In conjunction with the lack of modern geochronological data, the tectonic significance of the Balsfjord Series as it is defined today remains largely unclear.

3. Succession of deformation structures

During structural mapping, a total of four deformation events were identified and labelled as D_{0-1}, D_2, D_3 and D_4. All the events are considered as progressive (cf. Fossen et al., 2019), and their numbering is related to the pervasive fabric bearing the peak metamorphic mineral assemblage and labelled as S_2.

On some occasions where the metamorphic grade in the Balsfjord Series is low or the main metamorphic foliation S_2 is not pervasive, an original S_{0-1} fabric can be observed, which is defined as an original sedimentary bedding S_0, or other sedimentary structures that are with various intensity transposed into an incipient metamorphic foliation S_1. Since the transition between the S_0 and S_1 is difficult to distinguish in the field, they are both labelled as one fabric S_{0-1}. The S_{0-1} fabric becomes folded by F_2 folds with subhorizontal to gently inclined fold axial planes (sub)parallel to the surrounding main metamorphic fabric S_2. Hinges of the F_2 folds are in most of the cases parallel to the stretching lineation Ls_2 developed on S_2 foliation planes (Figs. 2, 3 and 4f). D_3 is only observed as a local feature throughout the area. It is characterized by folding of both the main metamorphic fabric S_2 and Ls_2 by F_3 folds with moderately inclined to flat axial planes (Figs. 5 and 6a).

The D_4 deformation overprints the entire regional fabric by steeply inclined to upright F_4 folds or a spaced S_4 cleavage with increasing intensity towards the contact of the Balsfjord Series with the LMC (Figs. 2, 5 and 6). Both D_3 and D_4 structures overprint earlier fabrics, but they are distinguished based on different orientations, style of folding as well as occurrence throughout the area.

Due to its structural complexity, the Balsfjord Series has been subdivided into three structural domains (A, B and C) described in detail below. Figs. 2, 5 and 7 contain measurements showing fold orientations together with planar fabrics and stretching lineations corresponding to the nomenclature described above and include cross-sections through the respective area. Furthermore, each domain has been subdivided into two or three regions and associated stereoplots show the above-mentioned fabrics ranging from D_{0-1} to D_4. Structural data (Figs. 2, 5 and 7) are shown as lower hemisphere equal area projection stereoplots of lineations and poles to planar features and contouring was calculated by the modified Kamb method at 5 levels of equally distributed density in the software Orient (Vollmer, 1995, 2015).

3.1. Domain A – Malangen peninsula to Storsteinnes/Svartnes

Region A1 in the NW of the domain shows a S_2 metamorphic fabric that is usually subhorizontal or dipping gently towards the SW or NE. In the NW part of the Malangen peninsula the Ls_2 lineation is plunging gently towards NW–SE or NNW–SSE as it is commonly described for the North Norwegian Caledonides (e.g., Faber et al., 2019; Ceccato et al., 2020). The S_2 foliation contains domains with F_2 folds showing axial planes gently dipping WSW and subhorizontal NW–SE trending F_2 fold axes that are parallel to the Ls_2 (Figs. 2, 3 and 4a). Generally, F_2 folds reflect varying strain (Fig. 4), as seen in quartzite bodies that exhibit.

steep, thick S_{0-1} limbs representing moderate strain, together with higher-strain, flat limbs that are (sub)parallel with the metamorphic foliation S_2 (Fig. 4b). The shear sense indicators in this region consistently show top-to-the SE direction of movement (Fig. 4c). Along the coastline further towards SE in region A2, the steep cleavage of S_4 becomes more prominent (Fig. 2). Occasionally, it is possible to see the entire succession of the deformation sequence, where the earliest S_{0-1} fabric is folded by isoclinal S_2/F_2 folds which are finally overprinted by the steep S_4 cleavage or upright F_4 folds (Fig. 4d). F_2 fold axes are concentrated in NW–SE orientations similar to the stretching lineation Ls_2 (Fig. 2), which shows a minor anticlockwise reorientation in comparison to region A1 (cf. Fig. 2 upper left and Fig. 2 bottom left). Region A3 (Fig. 2 right) features rocks with generally lower grade than further W or NW, turning from typical garnet micaschists to chlorite schists or even slates in areas of very low-grade metamorphism S of Storsteinnes. Due to the comparatively weak rheology and generally weaker expression of D_2, distinct stretching lineations as well as fold axes orientations become increasingly difficult to trace in the lower tectonostratigraphic levels of the Balsfjord Series. In addition, S_4 is dominant close to the LMC leading to a high degree of interference between F_2 and F_4, as described by Bergh and Andresen (1985). It is still possible to trace the structures relatively well on the northern side of the fjord in e.g., Svartnes where some of the F_2 fold axes have been reoriented to an E–W direction (Fig. 2). This matches with the further anticlockwise rotation of the Ls_2 in this region also showing an E–W orientation, and kinematic indicators displaying top-to-the-E shear senses (Fig. 4e). Still further E towards Laksvatn the reorientation of the lineation becomes even more apparent with both the F_2 fold axes as well as the Ls_2 trending SW–NE, and kinematic indicators showing top-to-the-NE shear sense (Fig. 4g). The gradual reorientation of these two linear features is illustrated in Fig. 3 which shows the Ls_2 azimuth against the angular difference between the Ls_2 azimuth and the F_2 fold axis azimuth. Apart from five measurements all data lie within an angular difference of less than 20° and more than half of the measurements show a divergence of 10° or less illustrating that these two features remain virtually parallel throughout regions A1–A3.

The first profile presented at the bottom of Fig. 2 starts in the WTBC in the NW and continues towards the SE ending in the RNC. In the NW, the Balsfjord Series is shown as directly overlying the basement although the nappe stack here is offset by a regional Permian–Early Triassic high-angle normal fault (Bergh et al., 2007; Indrevær et al., 2014). The mostly horizontal foliation S_2 of the Balsfjord Series gradually becomes overprinted by the initially only locally developed axial planar S_4 cleavage (Fig. 2). The lower contact of the LMC represents the boundary with the Nordmannvik Nappe of the RNC and marks a major tectonic discontinuity in the area (Faber et al., 2019). The second profile is drawn across the Malangen peninsula and illustrates the large-scale F_2 folding that affected the Balsfjord Series and possibly the overlying Tromsø Nappe (Fig. 2 bottom; after Kristensen, 1983).

In summary, domain A shows a distinct counterclockwise reorientation of both the F_2 fold axes as well as the Ls_2 stretching lineation from originally NW–SE (up to N–S) to W–E and finally SW–NE orientations and these two linear features remain virtually parallel to each other across the entire domain (Fig. 3). The main metamorphic foliation S_2 is subhorizontal or gently dipping unless affected by the S_4 cleavage steeply dipping to either NW or SE. Initially, this cleavage is observed in the field as a weak, localized overprint together with corresponding crenulations trending NE–SW (Fig. 4d). Further to the SE however, it amplifies quickly reaching its highest intensity at the boundary with the underlying LMC (Fig. 6c–e).

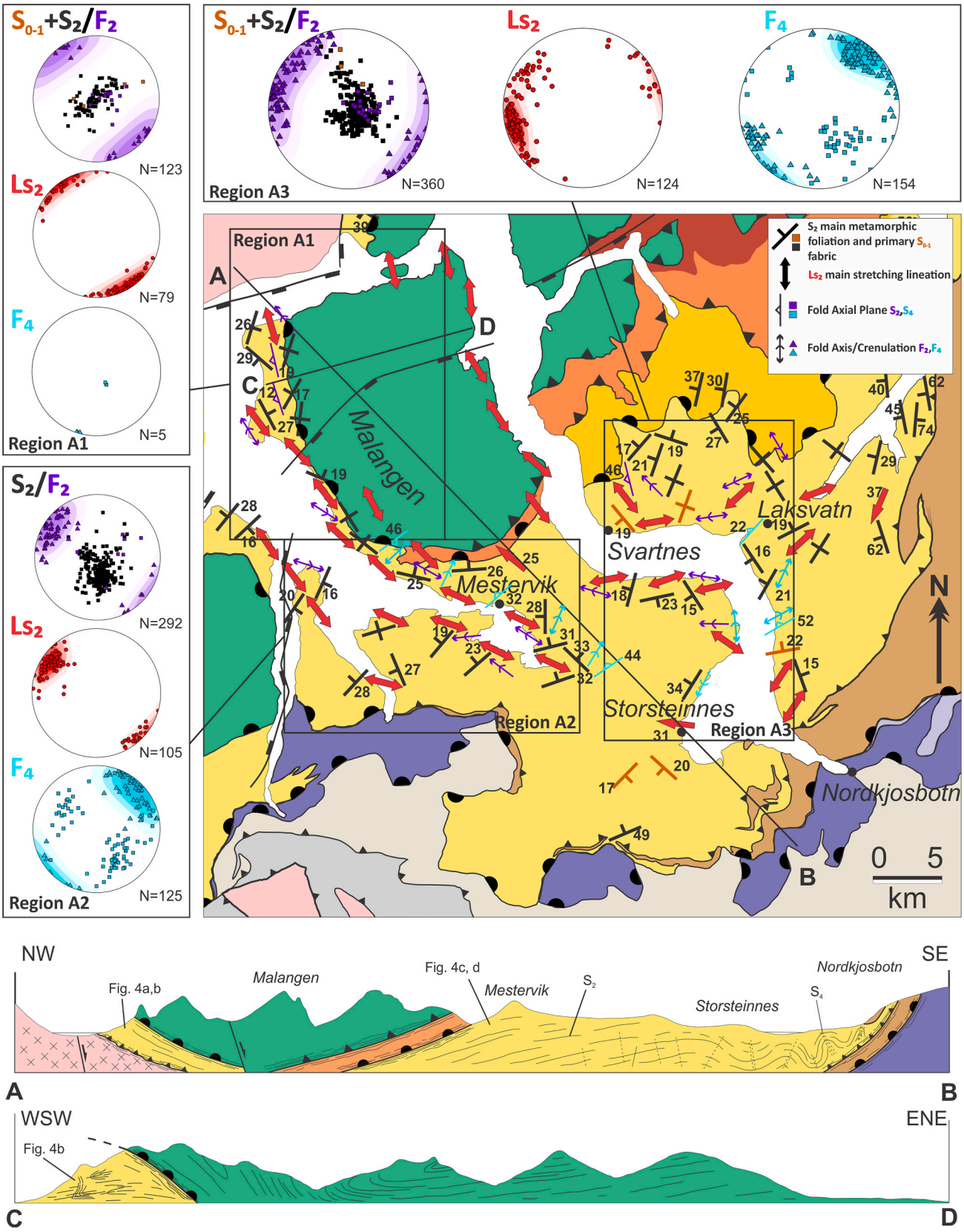

Fig. 2. Domain A located in the centre of the working area (Fig. 1) around Malangen peninsula. The area is subdivided into 3 regions (black rectangles). Each region features structural symbols and stereoplots (Vollmer, 1995, 2015) depicting the orientation of structures associated with different deformation events. The upper profile features 3.125 times exaggerated topography with layers displayed with their true/apparent dip (the same applies to Figs. 5 and 7). The lower profile is modified from Kristensen (1983) and illustrates the large-scale F_2 folding.

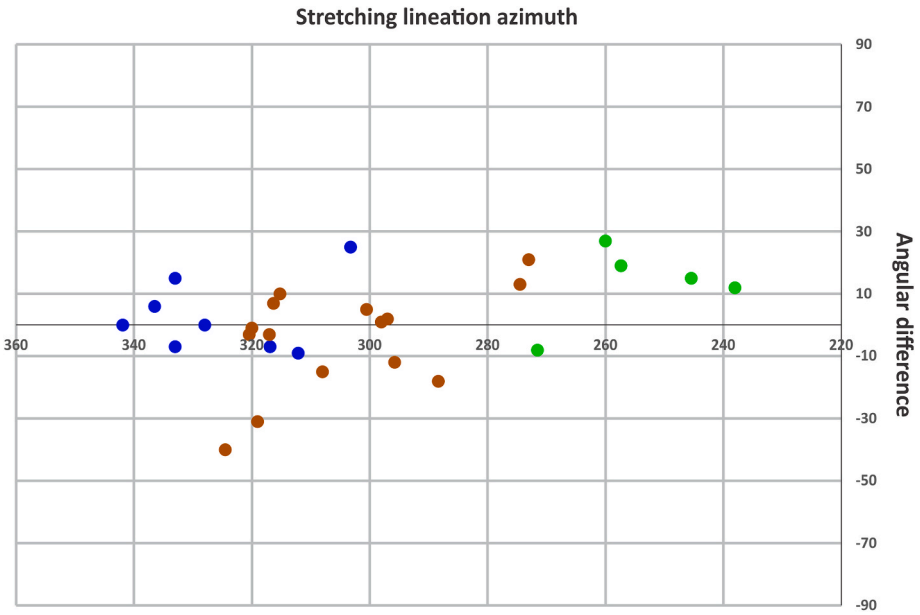

Fig. 3. Plot showing the angular difference between the stretching lineation azimuth and the fold axis azimuth in domain A plotted both clockwise (90°) and anticlockwise (−90°) from the lineation azimuth on the y-axis versus the stretching lineation azimuth on the x-axis (360°/N to 220°/SW). Each datapoint plotted represents an outcrop where all the measured stretching lineations and fold axes were averaged and then compared in terms of their angular difference. The datapoints are grouped by color for each of the three subregions (blue A1, brown A2, green A3), illustrating how higher values on the x-axis generally correspond to regions further northwest while lower values correspond to regions further southeast.

3.2. Domain B – from Hansnes across Ullsfjord and south towards Laksvatn

At Hansnes in the north of Region B1 (Fig. 5, top) the main metamorphic foliation S_2 is folded together with the stretching lineation Ls_2 by moderately inclined, tight folds labelled F_3 (Fig. 6a). The S_3 axial planes show similar orientations but are substantially steepened with respect to the flat lying, regional S_2 foliation (Fig. 5 top and 6a). In terms of orientation of S_2, the situation on Reinøya is comparable to NW Malangen with both the fold axes F_2 and stretching lineation Ls_2 plunging NW–SE (Fig. 2 top left and Fig. 5 top). Shear senses also remain the same with top-to-the-SE directions (Fig. 6d) and the region only shows a weak S_4 overprint.

In region B2, the western part of Ullsfjord dominantly features the main fabric S_2 exhibiting typical flat orientations with a NW–SE trending stretching lineation while D_4 remains only locally developed. This area of region B2 also shows a local D_3 overprint manifested as crenulation bands that cut across the main foliation S_2 (Fig. 6g). These gently NW dipping structures display tight internal folding with SE directed vergence consistent with the NW–SE oriented Ls_2 (Fig. 6g). It is often possible to observe quartz-filled tension gashes which penetrate the S_2 and show a vertical orientation. Occasionally, these tension gashes are rotated or folded, and their reorientation is compatible with SE directed movement (Fig. 6g bottom). On the eastern side close to the LMC, the S_4 becomes dominant, appearing as axial planes of tight and upright F_4 folds and as a new planar fabric in domains of strongly developed S_4 cleavage (Fig. 6e). Along this eastern strip of the Balsfjord Series, the metamorphic grade is mostly low, so the $S_{0\text{-}1}$ is often still visible and mainly affected by the S_4, which occasionally features overprinting sets of cleavage planes (Fig. 6c). There are also signs of subhorizontal stretching in, or parallel with, hinges of the F_4 folds visible as a local stretching lineation in quartzites labelled as Ls_4 (Fig. 5 upper left). Region B3 of this domain is a northeastern continuation of the previously described region A3 (data from where the two overlap are plotted in both stereoplots). As in the corresponding part of domain A, it features a stretching lineation Ls_2 displaying both the common NW–SE trend as well as the reoriented W–E and SW–NE lineations. The F_2 fold axes follow the same trend, though they become increasingly obscured by the D_4 reworking in this region. The NNE–SSW directed stretching documented by the abovementioned secondary stretching lineation Ls_4, is expressed here as segmented hinges of F_4 folds (Fig. 6f). D_3 can be identified locally as folding of both the main fabric S_2 and the lineation Ls_2 (Fig. 5 left). The profile at the bottom of Figure.

5 ranges from the northwestern basement to the island of Reinøya across Ullsfjord and finally to the LMC in the E. The Caledonian nappes are again downfaulted by regional normal faults so a direct exposure of the contact between the Balsfjord Series and the basement is not visible in the profile but is exposed further north (Fig. 5). Further SE, the profile crosses Oldervik displaying the local D_3 overprint by crenulation bands (Fig. 6g) and continues through the Ullsfjord where D_4 starts as isolated cleavage planes that evolve into the dominant S_4 fabric further SE, which finally affects also the LMC (Fig. 6b).

In summary, domain B resembles domain A in terms of fabric development of D_4 and its gradual intensification towards the SE. However, there are no signs of the Ls_2 stretching lineation and F_2 fold axes being reoriented in a similar manner as is the case for the Malangen area. Instead, the S_2 fabric is locally folded by D_3 displaying variable orientations.

3.3. Domain C – from Skatvik through Finnsnes towards Malangen

Region C1 lies in the NE of domain C (Fig. 7) and extends almost up to NW Malangen (Fig. 2). In its eastern part, the S_2 is gently E-dipping to subhorizontal featuring a NW–SE trending stretching lineation Ls_2. Further S, the folding of the metamorphic fabric becomes more difficult to classify due to various orientations of fold axial planes and fold axes. There are relationships similar to NW Malangen with F_2 folds showing a steeper, thick $S_{0\text{-}1}$ limb together with a flat limb that is oriented parallel to the metamorphic foliation S_2 (Fig. 8a). However, the dominant quartzites of the area also show folds ranging from recumbent–isoclinal (Fig. 8b) to tight–gently inclined (Fig. 8c), which are difficult to assign to a deformation event. They exhibit high strains and appear to be folding

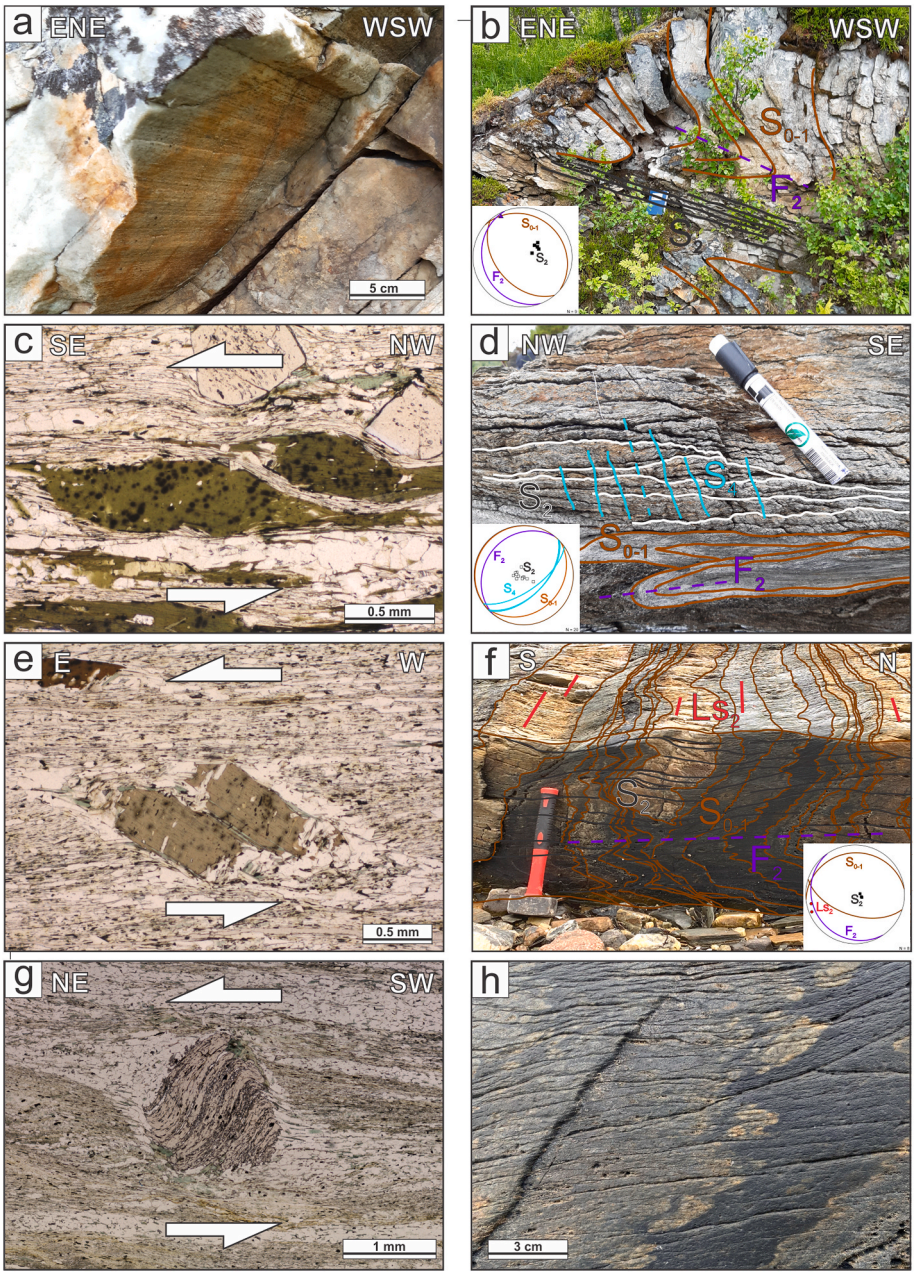

Fig. 4. A compendium of field and microscopic (ppl) photos illustrating the most important structural features in Domain A. a) Detail photo of Fig. 4b showing the well-developed Ls_2. Viewing direction is parallel to the F_2 fold axis (Region A1). b) S_{0-1} fabric in a quartzite with a steep, thick S_{0-1} limb and a flat and thinned limb aligned with S_2 (A1) c) Sigmoidal biotite indicating top-to-the-SE shear sense (A1). d) S_2 main foliation (highlighted in white) folding the earlier S_{0-1} fabric and being overprinted by the later S_4 spaced cleavage (A2). e) Bookshelf structure showing top-to-the-E shear sense (A3). f) Original bedding (S_{0-1}) overprinted by S_2 with distinct stretching lineation Ls_2 (A3). g) Garnet σ-clast displaying top-to-the-NE shear sense (A3). h) Close-up of a section of f) illustrating an example for preserved soft-sediment deformation structures in the form of load casts and flame structures (A3).

the metamorphic fabric of the quartzites as is the case for D_3, though without evidence for a folded stretching lineation. Where developed, the Ls_2 stretching lineation is trending NW–SE while fold axes orientations range from ENE to SSW (Fig. 7). In domains A and B, the orientations of F_2 fold axes are always parallel to the stretching lineation Ls_2 and the F_2 fold axial planes consistently dip WSW or are subhorizontal. In comparison, the fold axial planes in domain C have variable dip direction with flat–inclined axial planes. In addition, the high-strain and folding style matches more with the F_3 folds present in domain B. As a result, these folds are assigned to D_3 (Fig. 7 top). The final deformation event D_4 is rarely visible in this region (Fig. 7).

To the W of region C1, the Balsfjord Series overlies the basement with a moderately steep contact rarely preserved in other areas due to the extensive presence of post-Caledonian normal faults (Fig. 1). A short transect from the Balsfjord Series in the northernmost part of region C1 to the contact with the basement further southwest, reveals a strong increase in strain, culminating in a thin mylonitized horizon that marks the boundary between the two units. This contact can also be observed in the SW of region C2 (Skatvik), where it is possible to traverse the boundary between the two units with almost continuous exposure (Zwaan et al., 1998). The granitoid basement dips moderately steep and exhibits localized high-strain shear zones (Fig. 8d) or even a mylonitic.

fabric (Fig. 8e) within rocks otherwise showing no macroscopic Caledonian overprint. Samples from these local shear zones display top-to-the SE shear sense (Fig. 8h), which corresponds to the shear sense indicators of the overlying Balsfjord Series (Fig. 8f).

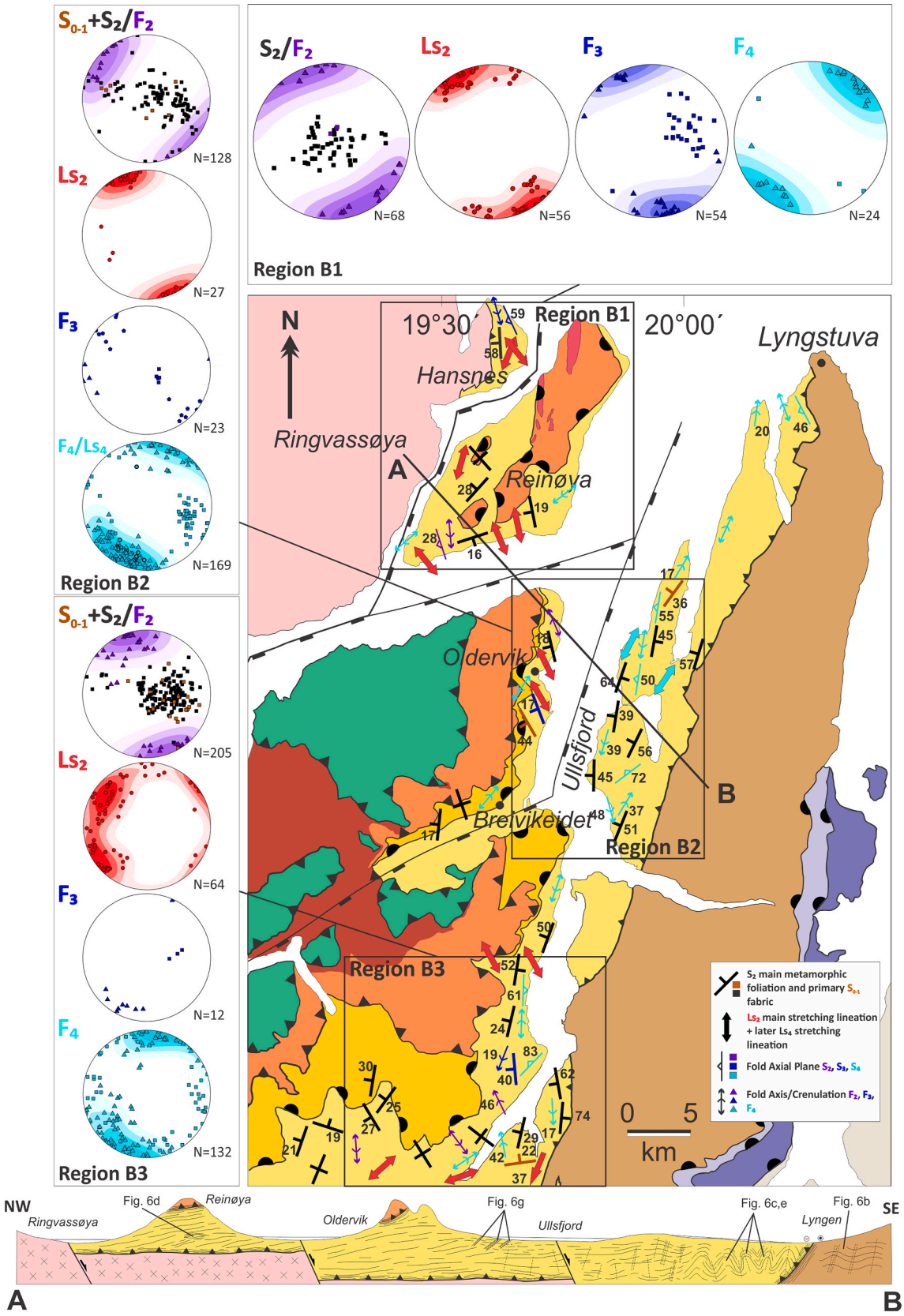

Fig. 5. Domain B located in the NE of the working area (Fig. 1) from S Ullsfjord to Reinøya and Hansnes. The area is subdivided into 3 regions (black rectangles). Each region features structural symbols and stereoplots (Vollmer, 1995, 2015) depicting the orientation of structures related to the different deformation events. Note the quartz veins (dark blue pentagons, B2) that crosscut the S_2 (Fig. 6g) and the late stage stretching lineation Ls_4 (light blue thick circles, B2).

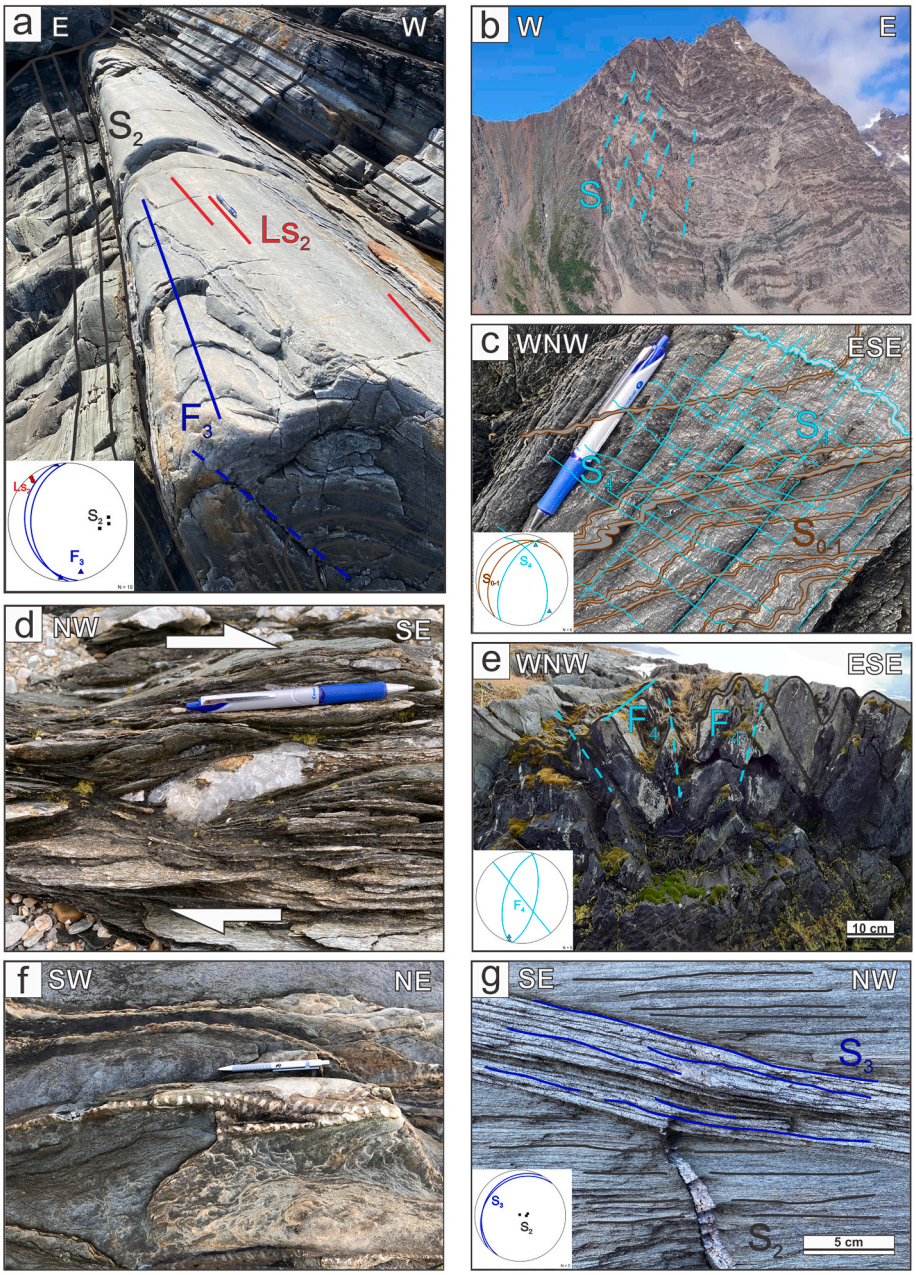

Fig. 6. Summary of key structural features in Domain B. a) Folding of the main metamorphic fabric S_2 by F_3 at Hansnes (Region B1). b) A flat fabric within the westernmost LMC affected by a steep cleavage possibly representing S_4. (B3, photo credit M. Galindos) c) Two steep axial planar cleavages (S_4) overprinting one another at E Ullsfjord (B2). d) Deformed quartz vein indicating top-to-the SE shear sense (B1) e) Steep to subvertical S_4 cleavage planes next to the Lyngen Gabbro (B2). f) Segmented carbonate vein documenting late-stage D_4 stretching (B3). g) Internally folded S_3 crenulation bands and quartz-filled tension gashes cross-cutting the main foliation S_2 (B2).

The cross-section at the bottom of Fig. 7 is drawn from the west of region C2 toward the W coast of Malangen. It illustrates the Balsfjord Series directly overlying the basement, which can only rarely be observed throughout the entire study area. The contact between the two units is first moderately steep but the S_2 fabric of the Balsfjord Series becomes flatter further E. This S_2 fabric is affected by gentle folding (Fareth, 1977) before dipping SE at the boundary to the overlying Tromsø Nappe. Further NE the entire sequence is affected by a normal fault before another nappe boundary appears between the Balsfjord Series and Tromsø Nappe that is again down-faulted in the E.

In summary, folds observed in domain C are more difficult to classify in terms of the $D_{0\text{-}1}$–D_4 nomenclature defined above. In the NE of the domain the orientation of the metamorphic fabric resembles the one in Malangen, but becomes increasingly obscure towards the SW. The most important aspect of domain C is the direct contact between the basement and the overlying Balsfjord Series at Skatvik in the SW. Local shear zones within the granitoid basement rocks show a NW–SE oriented stretching lineation with top-to-the SE shear senses matching the kinematic indicators of the Balsfjord Series.

4. Dating of shear zones within the Senja basement

As described in the previous section, the pre-Caledonian basement at Skatvik features local shear zones parallel with the S_2 fabric in the overlying Balsfjord Series (Fig. 8d and e). These shear zones contain local nests of titanite (Fig. 8g) associated with accumulations of biotite

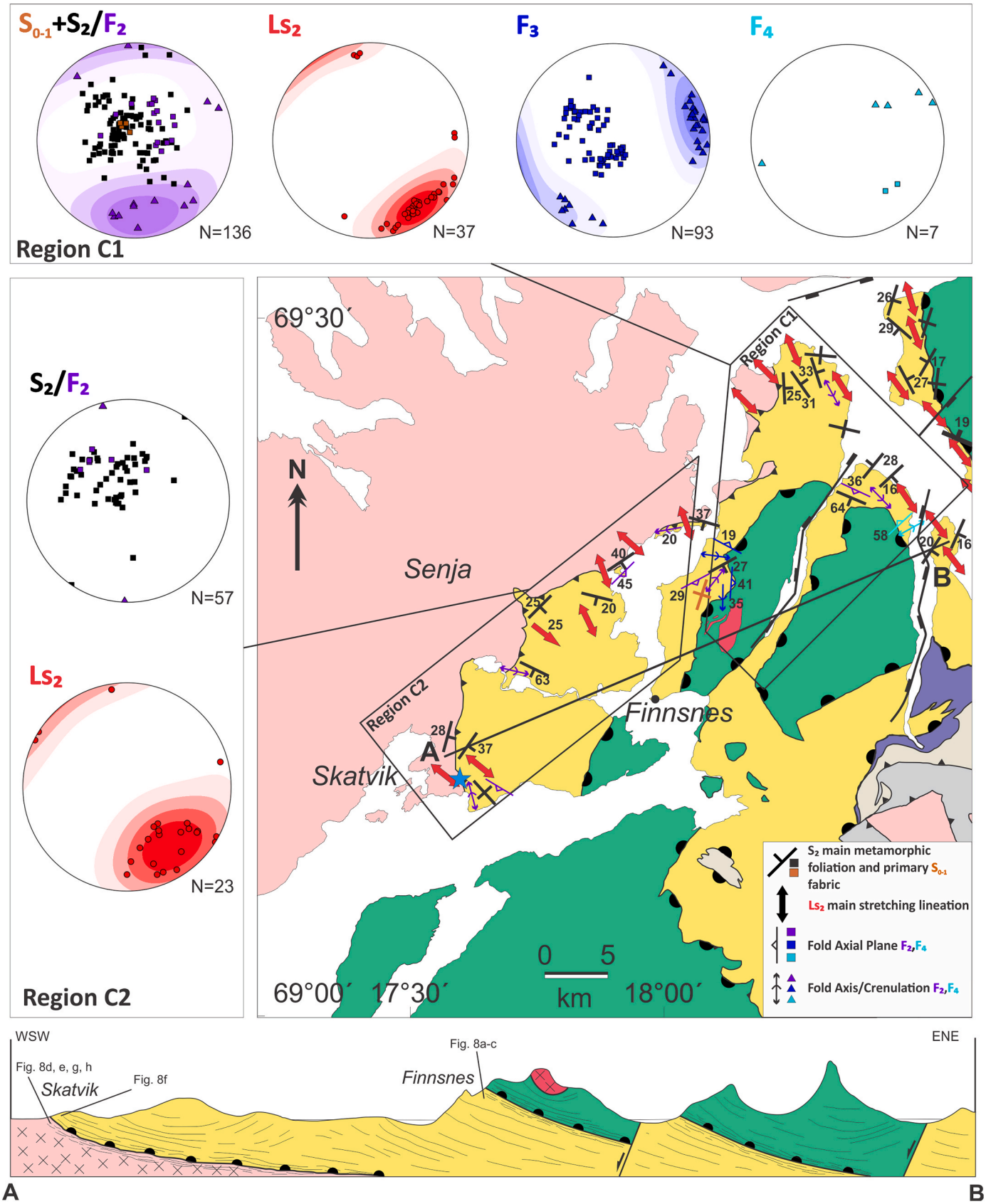

Fig. 7. Domain C located in the SW of the working area (Fig. 1) extending from Skatvik towards Finnsnes and ending close to NW Malangen. There are only two regions in this domain (black polygons). Each region features structural symbols and stereoplots (Vollmer, 1995, 2015) depicting the orientation of structures developed during the different deformation events. The blue star marks the location of the basement sample used for U–Pb dating of titanite (21–124); see Fig. 9.

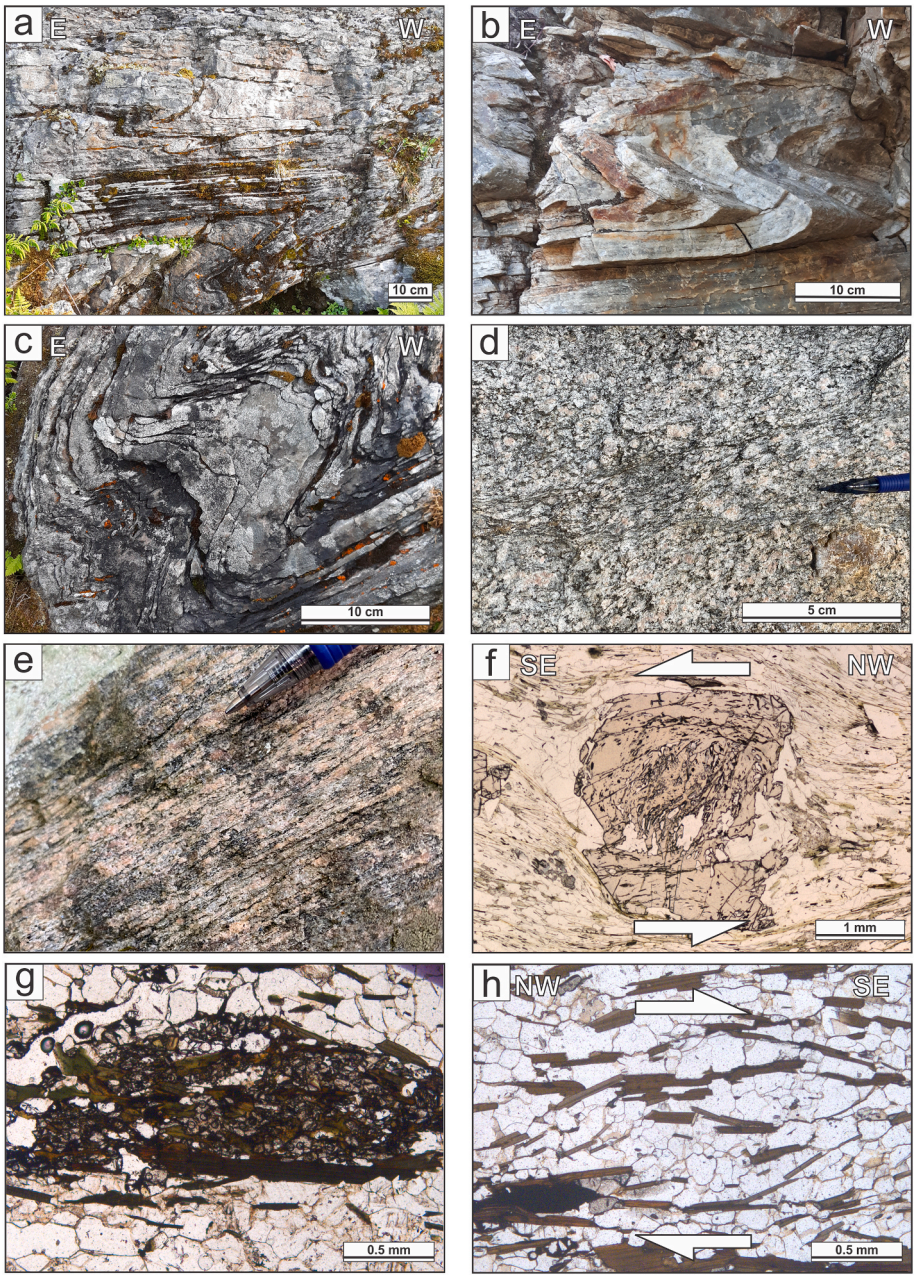

Fig. 8. A summary of important structural features of domain C. a) $S_{0\text{-}1}$ fabric with flat limbs of F_2 folds aligned with the main metamorphic foliation in the area, similar to NW Malangen (Fig. 4b, Region C1). b) Isoclinal-recumbent high-strain fold, folding the main metamorphic fabric S_2 (C1). c) Steeper fold within the local quartzites folding the main fabric S_2 (C1). d) Local shear zones within the basement at Senja (C2). e) Close-up of a high-strain shear zone in the Senja basement rocks (C2). f) Garnet σ-clast indicating top-to-the SE shear sense within the Balsfjord Series metapelites directly overlying the basement in the W (C2). g) Large accumulations of titanite in sample 21–124 (associated with biotite) in the local shear zones within the basement (C2). h) Sigmoidal shaped aggregate showing top-to-the-SE shear sense in local shear zones within the basement (C2).

and we interpret their crystallization as a result of Ti and Ca release from the biotite and plagioclase, respectively, during shearing of the host granitoid rocks (Fig. 8g). The sample 21–124 (Fig. 9) was collected next to the boundary between the WTBC and the Balsfjord Series in Skatvik (Fig. 7, blue star). U–Pb analysis of titanite was conducted in-situ on polished 30 μm-thin sections at the Institute of Geology of the Czech Academy of Sciences, Prague, Czech Republic. The analytical details are provided in Supplementary Tables (Tables 1 and 2).

The sample yielded an array of discordant U–Pb isotopic data showing variable proportion of common lead in the studied titanite (f_{207} (%), i.e. the proportion of common Pb is in the range between ca. 3–44% from the total Pb, Supplementary Table 1 (Kirkland et al., 2017). The calculation within the Tera–Wasserburg Concordia plot space shows a lower discordia intercept age at 429 ± 5 Ma (Fig. 9), which is interpreted as the timing of the titanite crystallization. The U–Pb data array represents a uniform titanite population with good statistics. The excess MSWD of 2.5 is caused by the analyses with higher proportion of common Pb (Fig. 9) generating larger spread of the corresponding $^{206}Pb/^{238}U$ ratios. Nevertheless, the detailed examination of the U–Pb data shows that the data point with the highest proportion of common lead (f_{207} = 44.3%) has also anomalous content of total Pb and Th compared to other titanite analyses (Supplementary Table 1). The ca. 1 order of magnitude higher contents compared to the average of the other analyses for both Pb and Th indicates this single analysis could have

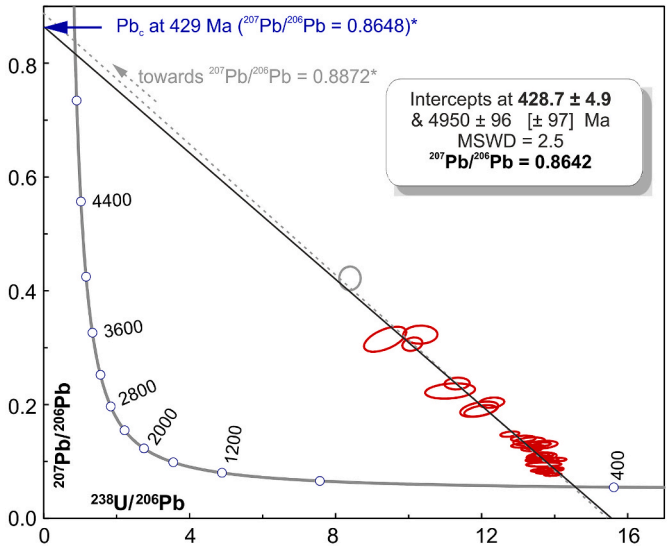

Fig. 9. Tera-Wasserburg plot showing the results of U–Pb titanite dating of the sample 21–124 taken from a localized shear zone within the WTBC close to the contact with the overlying Balsfjord Series (see Fig. 7 – blue star). For further explanations, see text.

been compromised by unintended ablation of a Pb–Th-rich inclusion. When this analysis is not taken into calculation (grey ellipse in Fig. 9), the discordia intercepts the ^{207}Pb/^{206}Pb at ca 0.8642, which is in perfect agreement with terrestrial common Pb composition of 0.8648 calculated for the age of 429 Ma using the equations of Stacey and Kramers (1975). When the analysis in question is taken into calculation, the array intercepts ^{207}Pb/^{206}Pb at a slightly higher ratio of ca. 0.8872. This discrepancy validates the removal of the analysis with highest content of common Pb from the calculation. The U–Pb data show a simple system where the radiogenic Pb is mixed with common Pb derived from the average terrestrial Pb reservoir and incorporated into titanite during its growth. There is no indication for any later alteration of the U–Pb system or Pb-loss in the studied titanite. The importance of this age for the regional interpretation of the study area is addressed in the following chapters.

5. Discussion

5.1. Development of deformation structures in the Balsfjord Series

The Balsfjord Series features a total of four sets of deformation structures ranging from $D_{0\text{-}1}$ to D_4, which we interpret as a result of a progressive deformation event that occurred at ca. 430 Ma.

5.1.1. $D_{0\text{-}1}$ and related structures

$S_{0\text{-}1}$ is interpreted to have formed during the onset of burial of the Balsfjord Series with a primary bedding S_0 gradually transposed into an incipient metamorphic fabric S_1 (Fig. 4b–d, f). Due to the presence of an inverted metamorphic gradient (e.g., Bergh and Andresen, 1985; Coker-Dewey et al., 2000), the southeastern part of the unit comprises a large area with low metamorphic grade (Menegon and Fagereng, 2021), featuring the best preserved $S_{0\text{-}1}$ fabric occasionally containing fossils (Binns and Matthews, 1981; Bjørlykke and Olaussen, 1981). This low-grade region extends from the south of Storsteinnes up to the northeast toward the southern Ullsfjord (Figs. 2 and 5). However, it is also possible to observe the $S_{0\text{-}1}$ in low-strain domains within areas dominated by the main fabric S_2 or the steep S_4. Examples can be found across Malangen in regions A1–A3 (Fig. 4b–f) where the subhorizontal S_2 overprinted the $S_{0\text{-}1}$. Region A3 occasionally also features preserved soft-sediment deformational structures like load casts and flame structures (Fig. 4h; e.g., Owen, 2003; Matsumoto et al., 2008). In the eastern parts of region B2 where the steep S_4 dominates, the $S_{0\text{-}1}$ is also occasionally preserved (Fig. 6c). Throughout these low-grade parts of the Balsfjord Series it is sometimes possible to observe boudinage structures, which we interpret to form during the $D_{0\text{-}1}$ deformation. These boudinaged layers show non-systematic orientation of stretching directions ranging from NE–SW to NW–SE.

5.1.2. D_2 structures

The metamorphic fabric S_2 of the Balsfjord Series is interpreted to have formed during ongoing burial, which established peak metamorphic assemblages showing increasing metamorphic grade towards NW. In domains of low D_2 strain, the $S_{0\text{-}1}$ is folded by the F_2 folds with gently dipping to flat-lying S_2 fold axial planes (Fig. 4b–d, f). In most of the area, S_2 forms the main metamorphic fabric represented by a flat foliation unless affected by overprinting deformation structures (see below). The S_2 also features a subhorizontal stretching lineation Ls_2 that is oriented NW–SE in the western and northwestern parts of the study area where the rocks also show top-to-the SE shear senses, which is typical for the North Norwegian Caledonides (e.g., Ceccato et al., 2020; Faber et al., 2019). Such kinematics are also present in S_2 shear zones developed within the pre-Paleozoic granitoid basement otherwise unaffected by the Caledonian deformation (Fig. 8h). These shear zones have been dated at ca. 430 Ma (Fig. 9) and we interpret this age and the parallelism of the deformational fabric with S_2 in the.

overlying Balsfjord Series as evidence for a localized Caledonian overprint of the basement during burial and subsequent emplacement of the overlying thrust nappes at around 430 Ma.

The F_2 folds in the metasedimentary rocks of the Balsfjord Series are cylindrical and tighten with increasing strain. Early-stage F_2 folds preserve the $S_{0\text{-}1}$ fabric in the steep limbs and exhibit higher strain in limbs (sub)parallel with the surrounding subhorizontal S_2 foliation (Fig. 4b–f). With increasing strain, the F_2 folds become recumbent and isoclinal (Fig. 4d). These F_2 folds, which predominantly show gently WSW-dipping to subhorizontal fold axial planes, feature NW–SE-oriented fold axes that are parallel to the Ls_2 (Figs. 2, 3 and 4a). This orientation and character of F_2 folds cannot be explained by their initiation through SE-directed shearing and subsequent rotation of the hinges into parallelism with the regional stretching direction. Such an evolution usually results in a) regional pattern of variable fold hinge orientation with respect to the general stretching direction, and b) progressive fold tightening during hinge rotation, both as a function of increasing shear strain (e.g., Alsop, 1992; Yang and Nielsen, 1995; Xypolias and Alsop, 2014). Throughout the study area, the documented F_2 folds do not display any systematic tightening but show varying interlimb angles (see Fig. 4b–d, f). Our data also show that both the Ls_2 and F_2 fold axes remain virtually parallel and rotate together anticlockwise as they approach the Lyngen Gabbro body in the domain A (Fig. 3).

It is possible to explain the parallelism of the F_2 fold axes with the Ls_2 through the orientation of an original anisotropy, like sedimentary bedding or a folded $S_{0\text{-}1}$ fabric, where the anisotropy is steeply dipping in a direction largely perpendicular to the general stretching direction (Stünitz, 1991). One possibility to create such a pre-D_2 geometry would be an earlier deformation of the $S_{0\text{-}1}$ fabric of the Balsfjord Series by NE–SW directed compression causing development of folds with NW–SE oriented fold axes. A similar process of an earlier fabric influencing the Caledonian deformation phase has been documented further E of the study area in the KNC (Ceccato et al., 2020) where the fold axes are also parallel to the general stretching lineation. Although the steep limbs of the early-stage F_2 folds (Fig. 4b–f) might be witnesses of such a folding event and other signs of it could have been obliterated during the development of pervasive S_2 fabric, there are no indications for such an event in the very low-grade parts of the Balsfjord Series, which show a comparatively weak and local D_2 overprint.

According to previous work in the WTBC (e.g., Bergh et al., 2010,

2015), the basement is characterized by an older, Svecofennian fabric with a dominant series of NW–SE trending folds created by NE–SW directed crustal shortening. It is feasible that these older structures influenced the early depositional fabric of the basin precursor to the Balsfjord Series in such a way that its marginal parts could have been made of strata inclined to NE or SW. Also, growth faults active during the opening of the "Balsfjord Basin", may have caused steepening of parts of the original sedimentary succession. As the Balsfjord Series was deformed during prograde burial and subsequent SE-directed Caledonian thrusting, the deformation could have produced F_2 folds with flat lying axial planes and fold axes parallel to the stretching lineation Ls_2 in regions where the original bedding was not (sub)horizontal.

5.1.3. D_3 structures

The D_3 structures are rare and interpreted as either local disturbances in the stress field during the D_2 shearing or as a result of heterogenous flow in the already established S_2. The former leads to F_3 folds that fold the main metamorphic fabric S_2 and the associated Ls_2, which is best observed in the north of domain B (Figs. 5 and 6a). In the central area of domain C, the F_3 folds.

show variable fold axes orientations (Fig. 7) that we also attribute to local variations of the stress field during ongoing D_2 shearing. Other structures like localized crenulation bands (Fig. 6g) or quartz-filled tension gashes (Fig. 6g and 5 - blue pentagons) form by heterogenous flow during D_2 as the previously developed S_2 is loaded during progressive southeast directed nappe stacking. Both types of structures are consistent with ongoing NW–SE stretching as described above (Fig. 2).

5.1.4. Rotation of Ls_2

Domain A in the Malangen area shows a gradual reorientation of the Ls_2 from its typical NW–SE orientation towards E–W and even NE–SW (Fig. 2). Based on our field data this pattern appears to be restricted to a certain structural horizon within the Balsfjord Series, which is expressed along the west coast of Malangen towards the E (see Fig. 2).

In the southeast, the Balsfjord Series is dominated by low grade metamorphic rocks like slates, limestones/dolomites or phyllites where the Ls_2 is either only locally developed or obscured by the increased presence of the D_4 deformation. However, earlier work by Bergh and Andresen (1985) studied conglomerates in the southeastern parts of domain A with trends ranging from NW–SE to WNW–ESE and E–W, concluding that the WNW–ESE orientation is likely the original stretching direction during D1 (our D_2 i.e. Ls_2) since it was only slightly affected by subsequent deformation phases. In addition, Andresen and Bergh (1985) described deformed conglomerates with X and Y axes lying in S1 (our S_2) and that they coincide with their F_1 fold axes (our F_2) when both could be measured. This matches well with our observations of the reorientation of the Ls_2 and F_2 fold axes although our explanation for this behaviour is not related to subsequent deformation (see below). Towards the north and structurally higher up, the Ls_2 reverts to its original NW–SE orientation, matching the typical orientation of the Ls_2 in other parts of the Balsfjord Series, as well as in the overlying Nakkedal and Tromsø nappes (Fig. 2).

A potential cause for the rotation of the stretching lineation Ls_2 would be folding of S_2 by a subsequent deformation event. However, if the main metamorphic foliation would be folded by an unrecognized event producing isoclinal folds in the S_2 foliation, the folded lineation would form either a girdle, or two maxima in the Schmidt-stereoplots each corresponding to one of the respective fold limbs. We do not observe neither (cf. Fig. 2), which is further corroborated by a PGR plot (Vollmer, 1990) quantifying the relationship between the distribution of linear and planar data (Fig. 10). It shows overlapping positions for S_2, Ls_2 and F_2 fold axes data close to P for regions A1 and A2. In area A3, the S_2 data still display a strong point maximum while the Ls_2 and F_2 fold axes are slightly shifted towards a girdle distribution. This is mostly related to the presence of some Ls_2 and F_2 measurements reverting to NW–SE in the N and NE of region A3 (Fig. 2). A folding-related girdle of

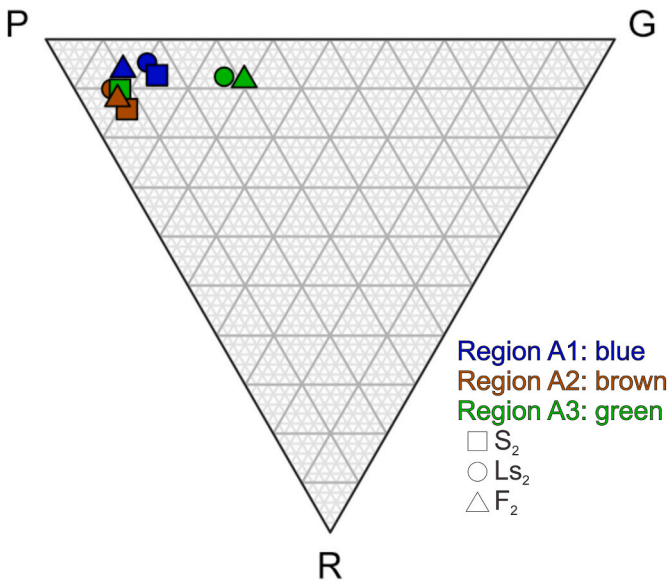

Fig. 10. PGR plot (Vollmer, 1990) to evaluate whether the linear and planar data in regions A1–A3 (Fig. 2) represent a point maximum (P), girdle (G) or whether they are randomly distributed (R). S_2: Foliation, Ls_2: Stretching lineation, F_2: Fold Axis.

sub-horizontal linear data with varying azimuth (i.e. areas A1–A3 in Fig. 2) could only be produced by folding of a horizontal lineation present on vertical surfaces.

Thus, the results above further support our interpretation that we see a gradual counterclockwise rotation of Ls_2 and F_2 fold axes within the S_2 fabric that maintains its sub-horizontal nature.

The orientation of the lineation on the folded surfaces could be also modified by ongoing shearing after the isoclinal folding, which could produce variable lineation directions on the subhorizontal foliation surfaces. However, it is unlikely that such situation would produce the observed regular pattern of lineations continuously rotating from NW–SE towards the NE–SW. If the reorientation would be caused by later folding through the steep, NE–SW striking F_4 folds, the folded Ls_2 would be steepened at least locally and should show variable plunge directions (see also e.g., Ghosh and Sengupta, 1987; Moosavi et al., 2014; Vitale et al., 2020). Neither of these can be observed in the study area and the Ls_2 and associated S_2 foliation retain their flat orientations throughout the entire area of lineation reorientation. This is also true for the F_2 fold axes that remain parallel to the stretching lineation and underwent a similar rotation (Figs. 2 and 3) although this relationship becomes increasingly obscure as the D_4 intensifies toward the southeast.

Because the Ls_2 and the hinges of F_2 folds remain virtually parallel and the rotated linear features are restricted to one horizon in the rock column, we suggest that they rotated together in a horizontal "channel" within the Balsfjord Series. We interpret this event as coeval with respect to the formation of the Ls_2, since the rocks in the channel are being actively deformed throughout the rotation of the Ls_2, as is evident by the kinematics changing accordingly from top-to-the-SE to E and finally NE (Fig. 4c–e, g). Consequently, we do not see any evidence that the stretching lineation in this horizon within the Balsfjord Series rotated passively but interpret the pattern as a result of its progressive reorientation during D_2-related transport.

There have been numerous reports of oblique or orogen-parallel lineations in otherwise non-transpressional settings (Merle and Brun, 1984; Fossen, 1993; Peterson and Robinson, 1993; Northrup and Burchfiel, 1996; Jeřábek et al., 2007), with one example in the KNC of the North Norwegian Caledonides (Kirkland et al., 2006). In the latter case, Kirkland et al. (2006) argued for the formation of a N–S trending orogen-parallel stretching lineation developed through constrictional

strain. This stretching lineation corresponds to a lateral escape of the KNC and overlying Magerøy Nappe as they were thrust against Baltica during the Caledonian collision. Ceccato et al. (2020) later stated that for this to be true, both the orogen-perpendicular and the orogen-parallel lineation need to be broadly coeval, develop at similar P–T conditions and display consistent kinematics. We claim that in the Balsfjord Series all these criteria are fulfilled since we observe [1] a gradual, not sudden, rotation of the same stretching lineation, not two orthogonal ones (Fig. 2) and [2] kinematic indicators that show a changing sense of movement along with the reorientation of stretching lineations (Fig. 4). Studies by both Peterson and Robinson (1993) and Kirkland et al. (2006) display the importance of the changes in transport direction they observe as a result of the emergence of a stronger rigid body that influences or prevents ongoing flow. We argue for a similar configuration in the case of the Balsfjord Series.

It should be noted that the Ls_2 rotated in a counterclockwise manner although the present-day geometry of the boundary between the Balsfjord Series and the LMC strikes mostly NNE–SSW and thus would favor a clockwise rotation during SE directed transport (Fig. 2). We explain this behavior as a result of the presence of a large, rheologically strong barrier that prevented flow towards the SE and instead redirected it into a northeastern direction. The only candidate to provide such a barrier would be the Mauken Window, which appears as a window of basement rocks in the southeast of the study area (Fig. 1) and acted as an indenter during the final stages of the continental collision. Another formation that plays a significant role here is the gabbroic body of the LMC limiting the movement of the Balsfjord Series toward the east. Without neither of these two units in the area, all the flow would likely be top-to-the-SE as is the case for the RNC in the east (Faber et al., 2019).

5.1.5. D_4 structures

The main fabric S_2 gradually steepens from the W towards the E as it is documented in domains A and B (Figs. 2 and 5), and we interpret this pattern as a large-scale manifestation of the D_4 folding. This deformation phase is first observed in outcrops as isolated domains of steep cleavages and crenulations overprinting the S_2 (Fig. 4d). Further toward the LMC, the S_2 (or in the southeastern part the $S_{0\text{-}1}$) planar fabric becomes continuously more affected until it is only locally encountered in its original flat orientation. Along the LMC, the $S_{0\text{-}1}$ and S_2 fabrics are strongly overprinted by the steep D_4 cleavage and upright folding with F_4 fold axes trending parallel to the interface between the Balsfjord Series and the LMC (Fig. 5). We believe this steep S_4 cleavage is not only visible in the Balsfjord Series, but also propagates into the westernmost parts of the LMC (Fig. 6b). Due to this steady and continuous intensification of the D_4 deformation toward the LMC, we interpret it to be a result of the shortening of the Balsfjord Series against the rheologically competent gabbroic body. We also see reorientation of the S_4 fabric depending on the orientation of the strike of the boundary between the Balsfjord Series and the LMC. In the NE of the study area (Lyngstuva) the contact between the units briefly changes strike from NNE–SSW to NNW–SSE and both the F_4 fold axial planes as well as the F_4 fold axes also adopt a NNW–SSE trend (Fig. 5). Furthermore, we document stretching along the eastern edge of the Balsfjord Series (Figs. 6f and 5 top right), that we interpret as a result of localized transpressional slip along the interface between the Balsfjord Series and the LMC.

Rheologically, the metapelitic Balsfjord Series is considerably weaker than the mostly gabbroic LMC, which causes a continuous folding of the former as thrusting continues. A critical point in this evolution is the orientation of the LMC. Our results show a steep, sheared contact between the Balsfjord Series and the LMC except from its southernmost part where the LMC begins to thin out. It is unknown how or when the LMC was steepened, but we see its steep western boundary as a prerequisite for not only the reorientation of the Ls_2 toward the NE, but also the final D_4 deformation stage producing the steep–upright fabric that dominates the Balsfjord Series in its eastern and northeastern extension.

6. Tectonic evolution of the regional nappe assembly and possibility of two sutures

Recent works (e.g., Janák et al., 2012; Augland et al., 2014) interpret the nappe assemblage of the North Norwegian Caledonides from the lowermost KNC to the uppermost Tromsø Nappe as one uninterrupted sequence later affected by Permian–Early Triassic high-angle normal faults (Bergh et al., 2007; Indrevær et al., 2014). Our results together with the work of Faber et al. (2019) done further east in the RNC, reveal several issues with such interpretation. The first problem is tied to the major and sudden change in metamorphic grade between the Nordmannvik Nappe (700–780 °C, 9–11 kbar) as the uppermost unit of the RNC and the overlying lower parts of the Balsfjord Series (315–400 °C and 3.5 kbar; Bergh and Andresen, 1985; Menegon and Fagereng, 2021). This sharp contrast in P–T conditions between two units that are in direct contact in areas where the LMC body is not present anymore (Fig. 1), implies the presence of a major tectonic boundary along which the RNC was brought to significantly greater depths than the overlying Balsfjord Series at ca. 440–432 Ma (Faber et al., 2019). In the Ofoten area further south, a very similar metamorphic break has been described where the kyanite-sillimanite grade Kvernmo nappe underlies the greenschist-facies Øse nappe (Anderson et al., 1992). These two units are separated by the Øse-thrust which demarcates two nappe complexes that both feature an inverted metamorphic gradient (Anderson et al., 1992; Anderson and Barker, 1999) as is observed in our study area. (Fig. 1).

The second problem originates from the tectonostratigraphic position of the Balsfjord Series directly overlying the WTBC in the north (domain B) and southwest (domain C) of the study area where the units are not affected by the post-Caledonian normal faults (Figs. 5 and 7). Consequently, both the RNC and KNC are entirely absent in this region, which poses an issue if the nappe assemblage is envisioned as one uninterrupted sequence with the Baltica basement underneath the KNC. The direct contact between the Balsfjord Series and WTBC has been documented by several authors in the past (Fareth, 1977; Zwaan et al., 1998, 2009; Velvin et al., 2015), but was never discussed in terms of its tectonic implications. Our observations confirm this thrust contact (Fig. 7) and show the presence of top-to-the SE shear sense indicators developed in both units (Fig. 8f–h). In addition, the dating of titanite in shear zones of the basement (Fig. 8d, e, g) yielding 429 ± 5 Ma (Fig. 9), represents evidence for localized Caledonian deformation in the WTBC. These shear zones are located at the contact with the overlying Balsfjord Series and their dating provides the time of shearing along the boundary between the Balsfjord Series and the WTBC during the Caledonian thrusting. This age estimate is consistent with an $^{40}Ar/^{39}Ar$ hornblende cooling age of 432 ± 2 Ma in the Balsfjord Series (Dallmeyer and Andresen, 1992), which can also be interpreted to approximate the peak P–T conditions due to the closure temperature of hornblende at 500–550 °C, which matches the maximum metamorphic grade (garnet zone) in the unit (Andresen and Bergh, 1985; Bergh and Andresen, 1985; Coker-Dewey et al., 2000). In addition, a syn-tectonic granitic intrusion within the Balsfjord Series was dated at 425 ± 1 Ma by Augland et al. (2014). These ages collectively constrain the timing of Caledonian thrusting responsible for development of the main metamorphic fabric in the Balsfjord series at ca. 432–425 Ma.

The overlying Tromsø and Nakkedal nappes exhibit ages of peak metamorphism between 456 and 449 Ma (Selbekk et al., 2000; Corfu et al., 2003b; Fassmer et al., 2020). The Tromsø Nappe also underwent rapid exhumation resulting in partial melting at 451–450 Ma (Corfu et al., 2003b), which was followed by rapid cooling as shown by a hornblende cooling age of 448 Ma ±2 (Dallmeyer and Andresen, 1992). This suggests that the Tromsø Nappe was emplaced onto the Nakkedal Nappe shortly after both reached their respective peak metamorphism. After this high-grade nappe complex was established at ca. 450 Ma, it was not thrust onto the Balsfjord Series until considerably later at around 430 Ma, which appears to be the timing of its metamorphic peak.

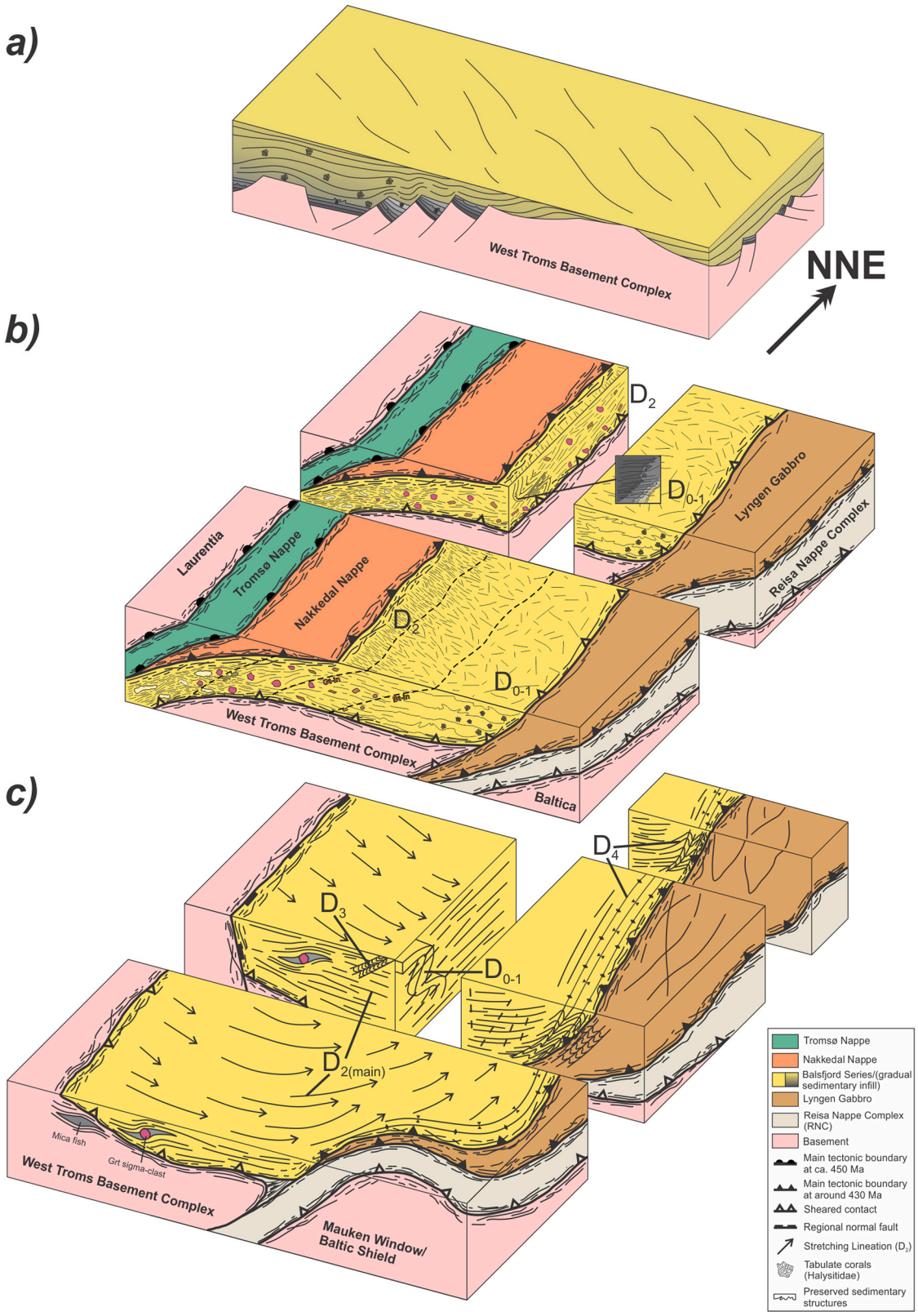

Fig. 11. Structural evolution of the Balsfjord Series illustrated in three stages. a) A possible scenario of deposition of the Balsfjord Series on the WTBC. The WTBC shows NW–SE striking tilted fault blocks that could lead to a steepening of the depositional fabric. b) Progressive burial of the Balsfjord Series and its underthrusting beneath the Tromsø and Nakkedal nappes. The detail inset represents the steepened $S_{0\text{-}1}$ as it is folded by S_2 (cf. Fig. 4h) c) Final stage of the continental collision and thrusting of the Balsfjord Series onto the WTBC. Note the rotation of the Ls_2 from NW–SE to E–W and finally NE–SW at this evolutionary stage. D_3 structures have developed locally, preceding the final structural overprint represented by D_4 which intensifies toward the Lyngen Magmatic Complex (LMC) and propagates into it. The overlying Tromsø and Nakkedal nappes are omitted.

The data presented above show that in terms of metamorphic ages, the evolution of the Balsfjord Series is contemporaneous with the evolution of the underlying RNC, whereas the Nakkedal and Tromsø nappes acted as an upper plate for the underthrusting of the Balsfjord Series and the WTBC. On the other hand, there is a major jump in metamorphic conditions between the Balsfjord Series as well as the LMC with respect to the underlying Nordmannvik Nappe of the RNC. This geological setting opens up the possibility for interpreting the tectonic evolution of the area as a result of the interaction between two sutures active at ca. 430 Ma (Fig. 11b). An alternative explanation for a similar metamorphic jump recorded between the Kvernmo nappe and the underlying the Øse nappe further south is large-scale out-of-sequence thrusting causing a major duplication of the nappe stack (Anderson et al., 1992). Adapting this interpretation would imply that the Tromsø and Nakkedal nappe as well as the Balsfjord Series are duplicates of the RNC and possibly the KNC further east. However, published data from these units (e.g., Corfu et al., 2003b; Janák et al., 2012; Kullerud et al., 2012; Faber et al., 2019; Ceccato et al., 2020; Fassmer et al., 2020) show that they feature different peak metamorphic ages as well as different P–T histories. As a result, we argue for a model featuring two sutures to explain the geological history of the study area.

7. Structural history of the Balsfjord Series as a three-stage model

The high variety of metasedimentary lithologies and clastic deposits comprising the Balsfjord Series indicate a continental and tectonically active depositional environment that was influenced by marine conditions (Bjørlykke and Olaussen, 1981; Andresen and Bergh, 1985; Andresen et al., 1985). The ridges within the WTBC seen in Fig. 11a illustrate the possibility for an older Svecofennian fabric with NW–SE trending folds caused by NE–SW directed crustal shortening (Bergh et al., 2010, 2015). This NW–SE oriented relief in combination with tilted fault blocks formed during active extension, could have led to an inclined fabric within the Balsfjord Series as deposition occurred (Fig. 11a). Such steepened strata potentially acted as a precursor fabric necessary to form F_2 fold axes parallel to the Ls_2 stretching lineation during Caledonian deformation.

Fig. 11b illustrates the gradual burial of the Balsfjord Series and development of its inverted metamorphic gradient. In its eastern parts the unit features the lowest metamorphic grade and the $S_{0\text{-}1}$ fabric, where some of the sedimentary structures and fossils are still preserved. As the unit is buried deeper towards the NW the F_2 folding begins to affect the $S_{0\text{-}1}$ fabric while the F_2 axial planar cleavage begins to develop. Occasionally, it is still possible to observe the sedimentary structures within the folded layers (detail inset in Figs. 11b and 4h). Still deeper, garnet eventually forms and the S_2 cleavage becomes a pervasive metamorphic foliation while in the deepest parts of the unit that we can observe today, staurolite starts to crystallize. This process is likely preceded by the arrival and attachment of a piece of oceanic crust (the Lyngen Magmatic Complex), but coeval with the development of the Reisa Nappe Complex, both in the tectonic footwall. At this stage, the S_2 fabric in the Balsfjord Series develops away from the LMC buttress. Fig. 11c shows the final stages of the structural evolution when the Balsfjord Series is thickened and exhumed from underneath the Nakkedal–Tromsø nappe assembly. This stage is coeval with arrival of the Baltica basement promontory represented by the Mauken Window. At this stage, the Ls_2 shows a strong reorientation along a structural horizon within the SE part of the Balsfjord Series, which is interpreted as a result of ongoing thrusting of the softer, mostly metapelitic rocks against the strong bodies of the LMC and the Mauken Window, both preventing continuous flow toward the SE. D_3 also develops during the thrusting stage and locally either folds the.

metamorphic fabric S_2 (Fig. 6a), or forms crenulation bands that cut across the foliation (Fig. 6g). D_4 is interpreted to represent the final movements of thrusting of the Balsfjord Series and the development of a steep S_4 cleavage that is extensively developed next to the LMC (Fig. 6e) and gradually fades out toward the west and northwest. A steep cleavage is also developed along the western edge of the LMC, which we interpret to be coeval with the S_4 cleavage in the Balsfjord Series (Fig. 6b).

8. Conclusions

Field and microstructural observations in the low–medium-grade metasedimentary Balsfjord Series in the upper part of the North Norwegian Caledonian nappe assembly can be summarized in the following key points.

1) The structural history features four deformation stages $D_{0\text{-}1}$–D_4, interpreted as a result of progressive burial of the Balsfjord Series and subsequent exhumation during thrusting. The progressive development of the main metamorphic fabric was associated with folding during various evolutionary stages, which we interpret either as a response to pre-existing anisotropies on the developing metamorphic fabric, or as a local perturbation of the prevailing stress field. The general top-to-the SSE–SE-directed transport is consistent with nappe translation observed in other parts of the North Norwegian Caledonides.
2) We have documented a gradual reorientation of the stretching lineation Ls_2 in the central region of the study area, which amounts to a total rotation of more than 90° from an originally NW–SE to E–W and finally NE–SW orientation. We interpret this feature as being present in a structural horizon within the Balsfjord Series in which transport was deflected toward the NE as the competent bodies of the Lyngen Magmatic Complex and the basement of the Mauken Window prevented further translation toward the SE. Ongoing push against the rigid Lyngen Complex backstop caused upright folding of the metasedimentary Balsfjord Series and development of a strong, steep cleavage in both units along their contact.
3) The timing of the progressive deformation affecting the Balsfjord Series is constrained by U–Pb age of 429 ± 5 Ma for titanite in the West Troms Basement Complex shear zones that are kinematically consistent with the overlying S_2 fabric in the Balsfjord Series micaschists. This age estimate is consistent with other geochronological investigations in the Balsfjord series.
4) Field observations confirmed a direct, sheared contact between the Balsfjord Series and the West Troms Basement Complex in areas not affected by the post-Caledonian high-angle normal faults. We suggest that the present-day assembly of geological units in the study area can be explained by the presence of a tectonic suture underneath the Lyngen Magmatic Complex along which the rocks of the Reisa and Kalak nappe complexes were deeply buried and later exhumed. This suture was active somewhat later (ca. 440–430 Ma) than the one responsible for the evolution and exhumation of the Tromsø and Nakkedal nappes at ca. 455–450 Ma. The latter suture must have been reactivated at ca. 430 Ma to allow for burial and exhumation of the Balsfjord Series at that time.

CRediT authorship contribution statement

Stephan M. Höpfl: Writing – review & editing, Writing – original draft, Visualization, Validation, Project administration, Methodology, Investigation, Formal analysis, Data curation, Conceptualization. **Jiří Konopásek:** Writing – review & editing, Writing – original draft, Visualization, Validation, Supervision, Resources, Project administration, Methodology, Investigation, Funding acquisition, Formal analysis, Data curation, Conceptualization. **Jiří Sláma:** Validation, Investigation, Formal analysis, Data curation.

Declaration of Generative AI and AI-assisted technologies in the writing process

During the preparation of this work the author(s) did not use any tool/service to assist in the creation of this article.

Declaration of competing interest

The authors declare that they have no known competing financial interests or personal relationships that could have appeared to influence the work reported in this paper.

Data availability

Data will be made available on request.

Acknowledgements

This article is part of a PhD project funded by UiT The Arctic University of Norway. J.S. was supported by the CAS support RVO 67985831. We would like to thank Holger Stünitz, Marina Galindos and Steffen Bergh for the numerous discussions and valuable input over the years. Marina Galindos also kindly provided the photo in Fig. 6b, which is highly appreciated. We also would like to thank Mark Anderson and Chris Kirkland for their constructive criticism and insight that improved the presentation of our work.

Appendix A. Supplementary data

Supplementary data to this article can be found online at https://doi.org/10.1016/j.jsg.2024.105102.

References

Alsop, G.I., 1992. Progressive deformation and the rotation of contemporary fold axes in the Ballybofey Nappe, north-west Ireland. Geol. J. 27, 271–283. https://doi.org/10.1002/gj.3350270305.

Andersen, T.B., Jamtveit, B., Dewey, J.F., Swensson, E., 1991. Subduction and eduction of continental crust: major mechanisms during continent-continent collision and orogenic extensional collapse, a model based on the south Norwegian Caledonides. Terra. Nova 3, 303–310. https://doi.org/10.1111/j.1365-3121.1991.tb00148.x.

Anderson, M., Barker, A., 1999. Caledonian Terrane Analysis in Troms-Tometrask, Northem Scandinavia, Utilizing the Geochemistry of High-Level Metabasites. NORSK GEOLOGISK TIDSSKRIFT.

Anderson, M.W., Barker, A.J., Bennett, D.G., Dallmeyer, R.D., 1992. A tectonic model for Scandian terrane accretion in the northern Scandinavian Caledonides. J. Geol. Soc. 149, 727–741. https://doi.org/10.1144/gsjgs.149.5.0727.

Andresen, A., Agyei-Dwarko, N.Y., Kristoffersen, M., Hanken, N.-M., 2014. A Timanian foreland basin setting for the late Neoproterozoic–Early Palaeozoic cover sequences (Dividal Group) of northeastern Baltica. Geological Society, London, Special Publications 390, 157–175. https://doi.org/10.1144/SP390.29.

Andresen, A., Bergh, S., 1985. In: GEE, D.G., STURT, B.A. (Eds.), Stratigraphy and Tectonometamorphic Evolution of the Ordovician-Silurian Balsfjord Group, Lyngen Nappe, North Norwegian Caledonides, pp. 579–592. The Caledonide.

Andresen, A., Fareth, E., Bergh, S., Kristensen, S.E., Krogh, E., Gee, D.G., Sturt, B.A., 1985. Review of Caledonian lithotectonic units in Troms, north Norway. The Caledonide Orogen-Scandinavia and Related Areas. John Wiley, New York, pp. 569–578.

Augland, L.E., Andresen, A., Gasser, D., Steltenpohl, M.G., 2014. Early Ordovician to Silurian evolution of exotic terranes in the Scandinavian Caledonides of the Ofoten–Troms area – terrane characterization and correlation based on new U–Pb zircon ages and Lu–Hf isotopic data. Geological Society, London, Special Publications 390, 655–678. https://doi.org/10.1144/SP390.19.

Bauville, A., Epard, J.-L., Schmalholz, S.M., 2013. A simple thermo-mechanical shear model applied to the Morcles fold nappe (Western Alps). Tectonophysics 583, 76–87. https://doi.org/10.1016/j.tecto.2012.10.022.

Beaumont, C., Jamieson, R.A., Nguyen, M.H., Lee, B., 2001. Himalayan tectonics explained by extrusion of a low-viscosity crustal channel coupled to focused surface denudation. Nature 414, 738–742. https://doi.org/10.1038/414738a.

Bellahsen, N., Jolivet, L., Lacombe, O., Bellanger, M., Boutoux, A., Garcia, S., Mouthereau, F., Le Pourhiet, L., Gumiaux, C., 2012. Mechanisms of margin inversion in the external Western Alps: implications for crustal rheology. Tectonophysics 560–561, 62–83. https://doi.org/10.1016/j.tecto.2012.06.022.

Bergh, S.G., Andresen, A., 1988. Reply to dallmeyer. Norw. J. Geol. 61, 70.

Bergh, S.G., Andresen, A., 1985. Tectonometamorphic evolution of the allochthonous caledonian rocks between malangen and Balsfjord, Troms, north Norway. Bull. - Norges Geol. Undersokelse 1–34.

Bergh, S.G., Corfu, F., Priyatkina, N., Kullerud, K., Myhre, P.I., 2015. Multiple post-Svecofennian 1750–1560 Ma pegmatite dykes in Archaean-Palaeoproterozoic rocks of the West Troms basement complex, north Norway: geological significance and regional implications. Precambrian Res. 266, 425–439.

Bergh, S.G., Eig, K., Kløvjan, O.S., Henningsen, T., Olesen, O., Hansen, J.-A., 2007. The Lofoten-Vesterålen continental margin: a multiphase Mesozoic-Palaeogene rifted shelf as shown by offshore-onshore brittle fault-fracture analysis. Norwegian Journal of Geology/Norsk Geologisk Forening 87.

Bergh, S.G., Kullerud, K., Armitage, P.E., Bouke Zwaan, K., Corfu, F., Ravna, E.J., Inge Myhre, P., 2010. Neoarchaean to svecofennian tectono-magmatic evolution of the West Troms basement complex, north Norway. Norwegian Journal of Geology/Norsk Geologisk Forening 90.

Binns, R.E., Matthews, D.W., 1981. Stratigraphy and Structure of the Ordovician-Silurian Balsfjord Supergroup. Troms, North Norway.

Bird, J.M., Dewey, J.F., 1970. Lithosphere Plate-continental margin tectonics and the evolution of the appalachian orogen. GSA Bulletin 81, 1031–1060. https://doi.org/10.1130/0016-7606(1970)81[1031:LPMTAT]2.0.CO;2.

Bjerkgård, T., Slagstad, T., Henderson, I.H., Sandstad, J.S., Schönenberger, J., 2015. Geology and gold mineralisation in the Mauken Precambrian basement window, Målselv, Troms, northern Norway. Norw. J. Geol. 95.

Bjørlykke, A., Olaussen, S., 1981. Silurian Sediments, Volcanics and Mineral Deposits in the Sagelvvatn Area. Troms, North Norway.

Boutoux, A., Bellahsen, N., Lacombe, O., Verlaguet, A., Mouthereau, F., 2014. Inversion of pre-orogenic extensional basins in the external Western Alps: structure, microstructures and restoration. J. Struct. Geol. 60, 13–29. https://doi.org/10.1016/j.jsg.2013.12.014.

Ceccato, A., Menegon, L., Warren, C.J., Halton, A.M., 2020. Structural and metamorphic inheritance controls strain partitioning during orogenic shortening (Kalak Nappe Complex, Norwegian Caledonides). J. Struct. Geol. 136, 104057 https://doi.org/10.1016/j.jsg.2020.104057.

Cloos, E., 1946. Lineation: A Critical Review and Annotated Bibliography. Geological Society of America.

Coker-Dewey, J., Steltenpohl, M.G., Andresen, A., 2000. Geology of western Ullsfjord, North Norway, with emphasis on the development of an inverted metamorphic gradient at the top of the Lyngen Nappe Complex. Nor. Geol. Tidsskr. 80, 111–118. https://doi.org/10.1080/002919600750042609.

Corfu, F., Andersen, T.B., Gasser, D., 2014a. The Scandinavian Caledonides: main features, conceptual advances and critical questions. Geological Society, London, Special Publications 390, 9–43. https://doi.org/10.1144/SP390.25.

Corfu, F., Armitage, P.E., Kullerud, K., Bergh, S.G., 2003a. Preliminary U-Pb geochronology in the West Troms basement complex, north Norway: archaean and palaeoproterozoic events and younger overprints. NORGES GEOLOGISKE UNDERSOKELSE 441, 61–72.

Corfu, F., Gasser, D., Chew, D.M., 2014b. New perspectives on the Caledonides of Scandinavia and related areas: introduction. Geological Society, London, Special Publications 390, 1–8. https://doi.org/10.1144/SP390.28.

Corfu, F., Ravna, E.J.K., Kullerud, K., 2003b. A late ordovician U?Pb age for the Troms? Nappe eclogites, uppermost allochthon of the scandinavian Caledonides. Contrib. Mineral. Petrol. 145, 502–513. https://doi.org/10.1007/s00410-003-0466-x.

Dallmeyer, R.D., 1992. 40Ar/'39Ar mineral ages within the Western Gneiss Terrane, Troms, Norway: evidence for polyphase Proterozoic tectonothermal activity (svecokarilian and sveconorwegian). Precambrian Res. 57, 195–206. https://doi.org/10.1016/0301-9268(92)90002-6.

Dallmeyer, R.D., Andresen, A., 1992. Polyphase tectonothermal evolution of exotic caledonian nappes in Troms, Norway: evidence from 40Ar39Ar mineral ages. Lithos 29, 19–42. https://doi.org/10.1016/0024-4937(92)90032-T.

Dewey, J.F., Pitman, W.C., Ryan, W.B.F., Bonnin, J., 1973. Plate tectonics and the evolution of the alpine system. GSA Bulletin 84, 3137–3180. https://doi.org/10.1130/0016-7606(1973)84<3137:PTATEO>2.0.CO;2.

Escher, A., Beaumont, C., 1997. Formation, burial and exhumation of basement nappes at crustal scale: a geometric model based on the Western Swiss-Italian Alps. J. Struct. Geol. 19, 955–974. https://doi.org/10.1016/S0191-8141(97)00022-9.

Faber, C., Stünitz, H., Gasser, D., Jeřábek, P., Kraus, K., Corfu, F., Ravna, E.K., Konopásek, J., 2019. Anticlockwise metamorphic pressure–temperature paths and nappe stacking in the Reisa Nappe Complex in the Scandinavian Caledonides, northern Norway: evidence for weakening of lower continental crust before and during continental collision. Solid Earth 10, 117–148. https://doi.org/10.5194/se-10-117-2019.

Fareth, E., 1977. Tranøy (Finnsnes). Berggrunnskart. Tranøy 1, 14333, 50 000; sort/hvitt.

Fassmer, K., Martinet, I., Miladinova, I., Sprung, P., Froitzheim, N., Fonseca, R.O.C., Münker, C., Janák, M., Kullerud, K., 2020. Lu–Hf geochronology of ultra-high-pressure eclogites from the Tromsø-Nappe, Scandinavian Caledonides: evidence for rapid subduction and exhumation. Int. J. Earth Sci. 109, 1727–1742.

Fossen, H., 1993. Linear fabrics in the Bergsdalen Nappes, southwest Norway: implications for deformation history and fold development. Nor. Geol. Tidsskr. 73, 95–108.

Fossen, H., Cavalcante, G.C.G., Pinheiro, R.V.L., Archanjo, C.J., 2019. Deformation – progressive or multiphase? J. Struct. Geol. 125, 82–99. https://doi.org/10.1016/j.jsg.2018.05.006.

Gee, D.G., 1975. A tectonic model for the central part of the Scandinavian Caledonides. Am. J. Sci. 275, 468–515.

Gee, D.G., Fossen, H., Henriksen, N., Higgins, A.K., 2008. From the early paleozoic platforms of Baltica and Laurentia to the caledonide orogen of scandinavia and

Greenland. Episodes Journal of International Geoscience 31, 44–51. https://doi.org/10.18814/epiiugs/2008/v31i1/007.
Gee, D.G., Ladenberger, A., Dahlqvist, P., Majka, J., Be'eri-Shlevin, Y., Frei, D., Thomsen, T., 2014. The Baltoscandian margin detrital zircon signatures of the central Scandes. Geological Society, London, Special Publications 390, 131–155. https://doi.org/10.1144/SP390.20.
Gee, D.G., Sturt, B.A., 1985. The Caledonide Orogen: Scandinavia and Related Areas. John Wiley & Sons.
Ghosh, S.K., Sengupta, Sudipta, 1987. Progressive development of structures in a ductile shear zone. J. Struct. Geol. 9, 277–287. https://doi.org/10.1016/0191-8141(87)90052-6.
Herwegh, M., Pfiffner, O.A., 2005. Tectono-metamorphic evolution of a nappe stack: a case study of the Swiss Alps. Tectonophysics 404, 55–76. https://doi.org/10.1016/j.tecto.2005.05.002.
Indrevær, K., Stunitz, H., Bergh, S.G., 2014. On Palaeozoic–Mesozoic brittle normal faults along the SW Barents Sea margin: fault processes and implications for basement permeability and margin evolution. J. Geol. Soc. 171, 831–846. https://doi.org/10.1144/jgs2014-018.
Jamieson, R.A., Beaumont, C., 2011. Coeval thrusting and extension during lower crustal ductile flow – implications for exhumation of high-grade metamorphic rocks. J. Metamorph. Geol. 29, 33–51. https://doi.org/10.1111/j.1525-1314.2010.00908.x.
Janák, M., Krogh Ravna, E.J., Kullerud, K., Yoshida, K., Milovský, R., Hirajima, T., 2013. Discovery of diamond in the Tromsø nappe, scandinavian Caledonides (N. Norway). J. Metamorph. Geol. 31, 691–703. https://doi.org/10.1111/jmg.12040.
Janák, M., Ravna, E.J.K., Kullerud, K., 2012. Constraining peak P-T conditions in UHP eclogites: calculated phase equilibria in kyanite- and phengite-bearing eclogite of the Tromsø Nappe, Norway: UHP eclogite from the tromsø nappe, Norway. J. Metamorph. Geol. 30, 377–396. https://doi.org/10.1111/j.1525-1314.2011.00971.x.
Jeřábek, P., Stünitz, H., Heilbronner, R., Lexa, O., Schulmann, K., 2007. Microstructural-deformation record of an orogen-parallel extension in the Vepor Unit, west carpathians. J. Struct. Geol. 29, 1722–1743. https://doi.org/10.1016/j.jsg.2007.09.002.
Kirkland, C.L., Hollis, J., Danišík, M., Petersen, J., Evans, N.J., McDonald, B.J., 2017. Apatite and titanite from the Karrat Group, Greenland; implications for charting the thermal evolution of crust from the U-Pb geochronology of common Pb bearing phases. Precambrian Res. 300, 107–120. https://doi.org/10.1016/j.precamres.2017.07.033.
Kirkland, C.L., Daly, J.S., Eide, E.A., Whitehouse, M.J., 2006. The structure and timing of lateral escape during the Scandian Orogeny: a combined strain and geochronological investigation in Finnmark, Arctic Norwegian Caledonides. Tectonophysics 425, 159–189. https://doi.org/10.1016/j.tecto.2006.08.001.
Kiss, D., Duretz, T., Schmalholz, S.M., 2020. Tectonic inheritance controls nappe detachment, transport and stacking in the Helvetic nappe system, Switzerland: insights from thermomechanical simulations. Solid Earth 11, 287–305. https://doi.org/10.5194/se-11-287-2020.
Kristensen, S.E., 1983. Strukturgeologiske og petrologiske undersøkelser av de øverste tektonostratigrafiske enheter på Malangshalvøya, Troms, vol. 270. Hovedfagsoppgave Univ. i Tromsø.
Krogh, E.J., Andresen, A., Bryhni, I., Broks, T.M., Kristensen, S.E., 1990. Eclogites and polyphase P?T cycling in the caledonian uppermost allochthon in Troms, northern Norway. J. Metamorph. Geol. 8, 289–309. https://doi.org/10.1111/j.1525-1314.1990.tb00474.x.
Kullerud, K., Nasipuri, P., Ravna, E.J.K., Selbekk, R.S., 2012. Formation of corundum megacrysts during H2O-saturated incongruent melting of feldspar: P–T pseudosection-based modelling from the Skattøra migmatite complex, North Norwegian Caledonides. Contrib. Mineral. Petrol. 164, 627–641. https://doi.org/10.1007/s00410-012-0765-1.
Kullerud, K., Skjerlie, K.P., Corfu, F., de la Rosa, J.D., 2006. The 2.40Ga Ringvassøy mafic dykes, West Troms Basement Complex, Norway: the concluding act of early Palaeoproterozoic continental breakup. Precambrian Res. 150, 183–200. https://doi.org/10.1016/j.precamres.2006.08.003.
Kvassnes, A.J.S., Strand, A.H., Moen-Eikeland, H., Pedersen, R.B., 2004. The lyngen gabbro: the lower crust of an ordovician incipient arc. Contrib. Mineral. Petrol. 148, 358–379. https://doi.org/10.1007/s00410-004-0609-8.
Lindstrøm, M., Andresen, A., 1995. Rb-Sr dating of a syn-tectonic granite within the Lyngen Nappe Complex and its implications for late orogenic evolution of the Troms Caledonides. Nor. Geol. Tidsskr. 75, 31–36.
Lundmark, A.M., Corfu, F., Spürgin, S., Selbekk, R.S., 2007. Proterozoic evolution and provenance of the high-grade Jotun Nappe Complex, SW Norway: U–Pb geochronology. Precambrian Res. 159, 133–154. https://doi.org/10.1016/j.precamres.2006.12.015.
Marko, W.T., Barnes, C.G., Yoshinobu, A.S., Frost, C.D., Nordgulen, Ø., 2014. Geology, geochemistry and emplacement conditions of the Vega intrusive complex: an example of large-scale crustal anatexis in north-central Norway. Geological Society, London, Special Publications 390, 603–631. https://doi.org/10.1144/SP390.2.
Matsumoto, D., Naruse, H., Fujino, S., Surphawajruksakul, A., Jarupongsakul, T., Sakakura, N., Murayama, M., 2008. Truncated flame structures within a deposit of the Indian Ocean Tsunami: evidence of syn-sedimentary deformation. Sedimentology 55, 1559–1570. https://doi.org/10.1111/j.1365-3091.2008.00957.x.
McArthur, K.L., Frost, C.D., Barnes, C.G., Prestvik, T., Nordgulen, Ø., 2014. Tectonic reconstruction and sediment provenance of a far-travelled oceanic nappe, Helgeland Nappe Complex, west-central Norway. Geological Society, London, Special Publications 390, 583–602. https://doi.org/10.1144/SP390.3.
Menegon, L., Fagereng, Å., 2021. Tectonic pressure gradients during viscous creep drive fluid flow and brittle failure at the base of the seismogenic zone. Geology 49, 1255–1259. https://doi.org/10.1130/G49012.1.
Merle, O., 1998. Emplacement Mechanisms of Nappes and Thrust Sheets. Springer Science & Business Media.
Merle, O., 1989. Strain models within spreading nappes. Tectonophysics 165, 57–71. https://doi.org/10.1016/0040-1951(89)90035-8.
Merle, O., Brun, J.P., 1984. The curved translation path of the Parpaillon Nappe (French Alps). J. Struct. Geol. 6, 711–719. https://doi.org/10.1016/0191-8141(84)90010-5.
Merle, O., Guillier, B., 1989. The building of the Central Swiss Alps: an experimental approach. Tectonophysics 165, 41–56. https://doi.org/10.1016/0040-1951(89)90034-6.
Mohanty, S., Ramsay, J.G., 1994. Strain partitioning in ductile shear zones: an example from a Lower Pennine nappe of Switzerland. J. Struct. Geol. 16, 663–676. https://doi.org/10.1016/0191-8141(94)90117-1.
Moosavi, E., Mohajjel, M., Rashidnejad-Omran, N., 2014. Systematic changes in orientation of linear mylonitic fabrics: an example of strain partitioning during transpressional deformation in north Golpaygan, Sanandaj–Sirjan zone, Iran. J. Asian Earth Sci. 94, 55–67. https://doi.org/10.1016/j.jseaes.2014.07.003.
Myhre, P.I., Corfu, F., Bergh, S., 2011. Palaeoproterozoic (2.0–1.95Ga) pre-orogenic supracrustal sequences in the West Troms basement complex, north Norway. Precambrian Res. 186, 89–100. https://doi.org/10.1016/j.precamres.2011.01.003.
Northrup, C.J., Burchfiel, B.C., 1996. Orogen-parallel transport and vertical partitioning of strain during oblique collision, Efjorden, north Norway. J. Struct. Geol. 18, 1231–1244. https://doi.org/10.1016/S0191-8141(96)00040-5.
Olesen, O., Torsvik, T.H., Tveten, E., 1997. Basement structure of the continental margin in the Lofoten-Lopphavet area, northern Norway: constraints from potential field data, on-land structural mapping and palaeomagnetic data. Oceanogr. Lit. Rev. 12, 1478.
Oliver, G.J., Krogh, T.E., 1995. U-pb Zircon Age of 469+-5 Ma for a Metatonalite from the Kjosen Unit of the Lyngen Magmatic Complex, Northern Norway.
Owen, G., 2003. Load structures: gravity-driven sediment mobilization in the shallow subsurface. Geological Society, London, Special Publications 216, 21–34. https://doi.org/10.1144/GSL.SP.2003.216.01.03.
Paulsen, H.-K., Bergh, S.G., Palinkaš, S.S., Karlsen, S.E., Kolsum, S., Rønningen, I.U., Armitage, P.E., Nasuti, A., 2021. Palaeoproterozoic foreland fold-thrust belt structures and lateral faults in the West Troms Basement Complex, northern Norway, and their relation to inverted metasedimentary sequences. Precambrian Res. 362, 106304.
Peterson, V.L., Robinson, P., 1993. Progressive evolution from uplift to orogen-parallel transport in a late-acadian, upper amphibolite- to granulite-facies shear zone, south-central Massachusetts. Tectonics 12, 550–567. https://doi.org/10.1029/92TC00822.
Ramsay, J.G., Casey, M., Kligfield, R., 1983. Role of shear in development of the Helvetic fold-thrust belt of Switzerland. Geology 11, 439. https://doi.org/10.1130/0091-7613(1983)11<439:ROSIDO>2.0.CO;2.
Ratschbacher, L., Frisch, W., Neubauer, F., Schmid, S.M., Neugebauer, J., 1989. Extension in compressional orogenic belts: the eastern Alps. Geology 17, 404. https://doi.org/10.1130/0091-7613(1989)017<0404:EICOBT>2.3.CO;2.
Ravna, E.J.K., Roux, M.R.M., 2006. Metamorphic evolution of the T⌀nsvika eclogite, Troms⌀ nappe—evidence for a new UHPM province in the scandinavian Caledonides. Int. Geol. Rev. 48, 861–881. https://doi.org/10.2747/0020-6814.48.10.861.
Ravna, E.K., Zozulya, D., Kullerud, K., Corfu, F., Nabelek, P.I., Janák, M., Slagstad, T., Davidsen, B., Selbekk, R.S., Schertl, H.-P., 2017. Deep-seated carbonatite intrusion and metasomatism in the UHP Tromsø nappe, northern scandinavian caledonides—a natural example of generation of carbonatite from carbonated eclogite. J. Petrol. 58, 2403–2428. https://doi.org/10.1093/petrology/egy016.
Rice, A.H.N., 2014. Restoration of the External Caledonides, Finnmark, North Norway, vol. 390. Geological Society, London, Special Publications, pp. 271–299. https://doi.org/10.1144/SP390.18.
Roberts, D., 2003. The Scandinavian Caledonides: event chronology, palaeogeographic settings and likely modern analogues. Tectonophysics, Collisional Orogenesis in the Geological Record and Modern Analogues 365, 283–299. https://doi.org/10.1016/S0040-1951(03)00026-X.
Roberts, D., Gee, D.G., Sturt, B.A., 1985. An introduction to the structure of the Scandinavian Caledonides. The Caledonide Orogen–Scandinavia and Related Areas 1, 55–68.
Schulmann, K., Lexa, O., Štípská, P., Racek, M., Tajčmanová, L., Konopásek, J., Edel, J.-B., Peschler, A., Lehmann, J., 2008. Vertical extrusion and horizontal channel flow of orogenic lower crust: key exhumation mechanisms in large hot orogens? J. Metamorph. Geol. 26, 273–297. https://doi.org/10.1111/j.1525-1314.2007.00755.x.
Schulmann, K., Melka, R., Lobkowicz, M.Z., Ledru, P., Lardeaux, J.-M., Autran, A., 1994. Contrasting styles of deformation during progressive nappe stacking at the southeastern margin of the Bohemian Massif (Thaya Dome). J. Struct. Geol. 16, 355–370. https://doi.org/10.1016/0191-8141(94)90040-X.
Selbekk, R.S., Skjerlie, K.P., 2002. Petrogenesis of the Anorthosite Dyke Swarm of Tromsø, North Norway: Experimental Evidence for Hydrous Anatexis of an Alkaline Mafic Complex, vol. 43.
Selbekk, R.S., Skjerlie, K.P., Pedersen, R.B., 2000. Generation of anorthositic magma by H_2O-fluxed anatexis of silica-undersaturated gabbro: an example from the north Norwegian Caledonides. Geol. Mag. 137, 609–621. https://doi.org/10.1017/S0016756800004829.

Selverstone, J., 1988. Evidence for east-west crustal extension in the Eastern Alps: implications for the unroofing history of the Tauern window. Tectonics 7, 87–105. https://doi.org/10.1029/TC007i001p00087.

Slagstad, T., Pin, C., Roberts, D., Kirkland, C.L., Grenne, T., Dunning, G., Sauer, S., Andersen, T., 2014. Tectonomagmatic Evolution of the Early Ordovician Suprasubduction-Zone Ophiolites of the Trondheim Region, Mid-Norwegian Caledonides, vol. 390. Geological Society, London, Special Publications, pp. 541–561. https://doi.org/10.1144/SP390.11.

Stacey, J.S., Kramers, J.D., 1975. Approximation of terrestrial lead isotope evolution by a two-stage model. Earth Planet Sci. Lett. 26, 207–221. https://doi.org/10.1016/0012-821X(75)90088-6.

Stünitz, H., 1991. Folding and shear deformation in quartzites, inferred from crystallographic preferred orientation and shape fabrics. J. Struct. Geol. 13, 71–86. https://doi.org/10.1016/0191-8141(91)90102-O.

Termier, P., 1922. A la gloire de la terre: souvenirs d'un géologue. Desclée de Brouwer.

Thompson, A., Schulmann, K., Jezek, J., 1997. Extrusion tectonics and elevation of lower crustal metamorphic rocks in convergent orogens. Geology 25, 491–494. https://doi.org/10.1130/0091-7613(1997)025<0491:ETAEOL>2.3.CO;2.

Turner, J.P., 1995. Gravity-Driven structures and rift basin evolution: rio muni basin, offshore equatorial west Africa1. AAPG (Am. Assoc. Pet. Geol.) Bull. 79, 1138–1158. https://doi.org/10.1306/8D2B21FF-171E-11D7-8645000102C1865D.

Van Hinsbergen, D.J.J., Hafkenscheid, E., Spakman, W., Meulenkamp, J.E., Wortel, R., 2005. Nappe stacking resulting from subduction of oceanic and continental lithosphere below Greece. Geology 33, 325. https://doi.org/10.1130/G20878.1.

Velvin, M., Ihlen, P., Binns, R.E., Zwaan, K.B., 2015. Berggrunnskart Reinøya 1534-1, M 1: 50 000.

Vitale, S., Tramparulo, F.D., Cappuccio, F., Ciarcia, S., 2020. Brittle vs. ductile strain during the synorogenic exhumation of HP-LT rocks: an example from the Lungro-Verbicaro Unit mylonites (northern Calabria, Italy). J. Geodyn. 135, 101719 https://doi.org/10.1016/j.jog.2020.101719.

Vollmer, F.W., 2015. Orient 3: a New Integrated Software Program for Orientation Data Analysis, Kinematic Analysis, Spherical Projections, and Schmidt Plots, vol. 49. Geological Society of America Abstracts with Programs.

Vollmer, F.W., 1995. C program for automatic contouring of spherical orientation data using a modified Kamb method. Comput. Geosci. 21, 31–49.

Vollmer, F.W., 1990. An application of eigenvalue methods to structural domain analysis. GSA Bulletin 102, 786–791. https://doi.org/10.1130/0016-7606(1990)102<0786:AAOEMT>2.3.CO;2.

Xu, Z., Wang, Q., Pêcher, A., Liang, F., Qi, X., Cai, Z., Li, H., Zeng, L., Cao, H., 2013. Orogen-parallel ductile extension and extrusion of the greater himalaya in the late oligocene and miocene. Tectonics 32, 191–215. https://doi.org/10.1002/tect.20021.

Xypolias, P., Alsop, G.I., 2014. Regional flow perturbation folding within an exhumation channel: a case study from the Cycladic Blueschists. J. Struct. Geol. 62, 141–155. https://doi.org/10.1016/j.jsg.2014.02.001.

Yang, Q., Nielsen, K.C., 1995. Rotation of fold-hinge lines associated with simple shear during southerly directed thrusting, Ouachita Mountains, southeastern Oklahoma. J. Struct. Geol. 17, 803–817. https://doi.org/10.1016/0191-8141(94)00112-D.

Zhong, Y., Kusky, T.M., Wang, L., Wang, C., Peng, Y., Wang, T., Yan, C., 2023. Alpine-style tectonic nappe stacking in an Archean suture zone: quantitative structural profile places constraints on orogenic architecture. Gondwana Res. 117, 86–116. https://doi.org/10.1016/j.gr.2023.01.007.

Zwaan, K.B., Fareth, E., Grogan, P.W., 1998. Geologisk Kart over Norge, Berggrunnskart Tromsø, M 1: 250.000. Norges Geologiske Undersøkelse.

Zwaan, K.B., Sødal-Pedersen, R.B., Kristensen, S.E., Landmark, K., 2009. Lenvik. Berggrunnskart; Lenvik; 14331; 1: 50 000; Foreløpig Utgave Plotteversjon.